University of
South-Eastern Norway

Mauricio Arturo Suncin Aguilar

Structural and shape changes on the fovea and outer retinal layers in Norwegian children ages 7 to 11

Master's Thesis

Masteroppgave -MPRO5001

2023

Department of Optometry,

Radiography, and Lighting

Design

University of South-Eastern Norway
Department of optometry, radiography, and lighting design
PO Box 4
3199 Borre Norway

http://www.usn.no

This thesis is worth 30 study points

Summary

This thesis investigated foveal morphology in 78 healthy Norwegian children aged 7-11 years using optical coherence tomography imaging. The study aimed to establish normative data on foveal width, depth, and outer retinal layer thickness in this pediatric cohort. Participants were evenly divided between males and females and two age groups, 7-8 years and 10-11 years. High-resolution scans of the macular region were obtained, and customized segmentation software extracted quantitative foveal dimensions for analysis. The parameters measured were foveal width, depth, outer nuclear layer thickness, axial length, spherical equivalent refraction, and corneal radius. Statistical comparisons were performed to assess sex and age-related differences. The results showed no significant differences in foveal width, depth, or outer nuclear layer thickness between males and females or between the younger and older groups. However, axial length was significantly longer in males compared to females. In conclusion, this study provides initial normative pediatric data on foveal structure in Norwegian children aged 7 to 11. Further large-scale longitudinal research is needed to fully elucidate developmental patterns over time. Establishing robust standards will help distinguish normal anatomical variation from potential pathology when clinically evaluating the pediatric fovea.

Keywords: fovea, optical coherence tomography, pediatric, retinal development, Norwegian

Sammendrag

Denne avhandlingen undersøkte foveal morfologi hos 78 friske norske barn i alderen 7-11 år ved hjelp av optisk koherens-tomografi (OCT) avbildning. Studiens mål var å etablere normative data for foveal bredde, dybde og tykkelse på det ytre netthinnelaget i denne pediatriske kohorten. Deltakerne var jevnt fordelt mellom gutter og jenter og to aldersgrupper, 7-8 år og 10-11 år. Høyoppløselige skanninger av makulaområdet ble innhentet, og spesialisert segmenteringsprogramvare ekstraherte kvantitative mål for foveal dimensjoner til analyse. De målte parametrene var foveal bredde, dybde, ytre kjerne lag tykkelse, aksial lengde, sfærisk ekvivalent brytning og hornhinnens radius. Statistiske sammenligninger ble utført for å vurdere forskjeller relatert til kjønn og alder. Resultatene viste ingen signifikante forskjeller i foveal bredde, dybde eller ytre kjerne lag tykkelse mellom gutter og jenter eller mellom de yngre og eldre gruppene. Imidlertid var aksial lengde signifikant lengre hos gutter sammenlignet med jenter. Avslutningsvis gir denne studien innledende normative data for pediatrisk foveal struktur hos norske barn i alderen 7 til 11 år. Videre storskala longitudinelle forskning er nødvendig for å fullt ut klarlegge utviklingsmønstre over tid. Etablering av robuste standarder vil hjelpe til med å skille normal anatomisk variasjon fra potensiell patologi ved klinisk vurdering av den pediatriske fovea.

Nøkkelord: fovea, optisk koherens-tomografi, pediatrisk, netthinneutvikling, norsk

Table of contents

Foreword

As a practicing optometrist who regularly assesses pediatric patients, understanding normal foveal development is directly relevant to my clinical interests. My background motivated me to pursue this research to help establish normal pediatric anatomy. The result of the analysis of this research will assist optometrists like myself in evaluating pediatric patients and contribute to evidence-based practice.

The realization of this master's thesis marks a significant milestone in my academic and personal journey. This journey has been both fulfilling and demanding at the same time.

I formally thank my academic advisor, Rigmor Baraas, for her guidance during research. I also acknowledge the University of Southern-Eastern Norway (USN) for providing the educational environment and resources that facilitated this research.

The emotional and psychological load of this journey cannot be overstated. Balancing the rigors of research with the responsibilities of family life has not been an easy task. My wife has been a constant source of support and understanding.

The experience of writing this thesis while raising a young family has taught me so much, and I have matured in the process. I began this mission with my son, who was just a year old when I started this research. Midway through, we welcomed the birth of my daughter, adding another layer of complexity and joy to the process. The late nights, the missed milestones, and the precious moments sacrificed for academic work will always live in my memory, giving the culmination of this research more meaning.

In retrospect, each keystroke and each moment spent looking over data and literature were also moments away from witnessing my children's laughter and my family's evolution. This thesis, therefore, is not just an academic document but a chronicle of a period in my life marked by immense growth and sacrifice.

To my family, especially my wife Rute and children Lars and Astrid, you are the heroes of this academic venture. Your support, large and small, has not gone unseen. This thesis is as much mine as yours.

Bergen, 2023

M. Arturo Suncin A.

1 Introduction

The fovea is responsible for critical visual functions and can be affected by many ocular conditions. Therefore, documenting the normal foveal developmental process is essential to differentiate it from pathological changes (Dubis et al., 2012). The pediatric fovea exhibits greater individual variability than individual adults, partially attributed to ongoing maturation (Ahn et al., 2005). Alterations to the normal developmental process can also produce abnormal foveal morphology linked to vision disorders (Bruce et al., 2013). The fovea has different characteristics that determine its size and shape; it is insufficient to analyze just the foveal thickness (Demir et al., 2022). Therefore, distinguishing normal anatomical variation from pathology requires understanding normal development patterns and establishing normative reference data with the population.

The importance of the retinal pigment epithelium (RPE) and its role in the foveal avascular zone (FAZ) is crucial to understanding the normal development of the foveal shape REF (Baraas et al., 2022). The normal development of the fovea and FAZ is quite a complex process; it begins prenatally, continues through infancy, and matures in adolescence. The FAZ begins forming around 25 weeks gestation as RPE cells secrete factors that prevent retinal vessels from growing into the area that will become the fovea (Provis, 2001). The FAZ is fully formed by term birth, around 40 weeks of gestation (Provis et al., 2013). Foveal pit formation occurs postnatally, enabled by the presence of the FAZ (Dubis et al., 2012). The inner retinal layers progressively thin, and a shallow pit becomes detectable around 2-4 months after birth as cone photoreceptors begin migrating centrifugally (Hendrickson et al., 2012). The foveal pit is formed by 15 - 24 months of age (Vajzovic et al., 2012). Foveal cone photoreceptors are immature at birth and undergo centrifugal migration to reach peak density in a small central area by adolescence (Provis et al., 2013).

The RPE role with the foveal shape is also essential. RPE pigmentation and secretion of growth factors are critical for normal cone differentiation and migration (Raviv et al., 201. Studies have found a strong correspondence between RPE and cone cell distributions and foveal morphology. This supports the hypothesis that the developmental role of RPE in guiding foveal cone formation has an impact on how foveal shape develops from birth through adolescence (Baraas et al., 2022).

Previous studies about the retina and fovea have mainly focused on general eye disorders or pathologies. Although the foveal structure is well-defined in adults, its development during childhood is not entirely understood. Still, there is a lack of data on how the fovea develops and changes in healthy children. Therefore, this study aims to fill this gap.

The Ocular Coherence Topography (OCT) provides a noninvasive means to track foveal development by imaging every retinal layer. Longitudinal OCT studies reveal a steady increase in foveal width and depth through childhood and adolescence, reflecting progressive foveal shape changes (Samara et al., 2015).

For this study, the OCT images have already been obtained as a part of a previous study (Suncin A., 2022). The dataset included children's health data; all collected data was anonymized. The informed consent from the children and their parents or guardians was collected when the OCT and other measures were taken. Children and parents got information about potential discomforts or harm caused by the data collection with the OCT. The scans were taken by Colour Vision and Retinal Imaging Research Group (CVRI) members using appropriate equipment and protocols.

Part of this thesis has been presented in the project protocol as the final exam in MRES019 Research Methods (Suncin A., 2022) at USN (unpublished).

Background

Anatomy

The adult anatomic macula has a diameter of approximately 4.5 to 6 mm, centered slightly temporal to the optic disc, and located between the superior and inferior temporal arcades (Bringmann et al., 2006; Hildebrand & Fielder, 2011; Thomas et al., 2022). The position of the center of the macula is slightly below the horizontal meridian of the eye; this feature is used to investigate the presence of cyclotorsional disorders when evaluating binocular problems in adults or children (Evans, 2009; Hildebrand & Fielder, 2011).

The fovea or anatomic fovea centralis lies in the center of the anatomic macula and consists of a slopeside pit named clivus (limits of the foveola), with a diameter of approximately 1.5 mm and a depth of 0.2mm in adults (Curcio et al., 1990; Hildebrand & Fielder, 2011). The fovea is responsible for numerous visual functions, such as high spatial resolution and color vision (Lee et al., 2015). The foveola at the base of the foveal pit contains a very high density of cone photoreceptors at approximately 199,000 cones/mm^2 (Curcio et al., 1990). The foveal cones are narrower and elongated compared to peripheral cones, allowing tighter packing to maximize the detection of light entering the central retina (Hendrickson et al., 2012; Hildebrand & Fielder, 2011). Foveal cone specialization depends on normal pit morphology, as abnormalities in foveal shape impair cone packing and vision (Tick et al., 2011).

The width of the fovea is the lateral distance between the nasal and temporal peak macular thickness, measured in microns. This measurement reflects the size of the foveal pit (Matsui et al., 2020), which is the depression in the center of the fovea, as discussed previously. The inner retinal layers are displaced from the foveola, which has the highest density of cone photoreceptor packing and gives rise to the distinctive foveal pit (Chui et al., 2012), additionally to the narrowing and elongation of the outer segment (OS) that allows the photoreceptors to create an arch called foveal bulge (Hasegawa et al., 2014). Foveal depth indicates the axial distance from the inner retinal surface to the retinal pigment epithelium (RPE) at the foveal base. Increased depth points to thicker foveal tissue, though not necessarily greater cone density (Staurenghi et al., 2014). A greater depth suggests a thicker foveal tissue but not necessarily a higher cone density in the foveal area (Lee et al., 2018).

Foveal diameter and slope geometry also refine postnatally, with diameter decreasing and pit walls steepening until maturity (Vajzovic et al., 2012; Yuodelis & Hendrickson, 1986). Histology shows that foveal elongation and remodeling of the inner retinal layers occur between fetal stages through the first postnatal years (Hendrickson et al., 2012). Foveal cone specialization depends on normal pit morphology, as abnormalities in foveal shape impair cone packing and vision (Tick et al., 2011). Table 1 summarizes foveal developmental milestones, diameter by age, pit depth by age, and ethnic variation through several studies.

Table 1 Summary fovea anatomy

Category	Age Range	Description	References
Foveal developmental milestones	Birth to 3 months	Immature, shallow foveal pit, retinal thickness decreased compared to the periphery. On OCT, the contrast between layers is more distinct than in adults. Shallow foveal pit present, IRLs thinned but persisted across fovea.	(Hendrickson & Yuodelis, 1984; Vajzovic et al., 2012)
	3 months to 2 years	Rapid increase in foveal pit depth, diameter decreases, slope walls steepen. ONL+HFL band thickness around the fovea. Rapid elongation of foveal IS and OS.	(Vajzovic et al., 2012; Yuodelis & Hendrickson, 1986)

	3 to 9 years	Gradual refinement of foveal shape, pit walls become steeper. The diameter narrows as cones pack densely. A marked increase in foveal ONL+HFL thickness from cone packing. ELM clearly separated from the IS band.	(Vajzovic et al., 2012; Wagner-Schuman et al., 2011)
	By 15 years	Foveal development is complete with adult-like anatomy. Thick foveal ONL, long IS, and OS. Thick Henle fiber layer visible on OCT.	
Foveal diameter by age	Newborns	Estimated at 0.32 to 0.53 mm. (Larger than adults 0.35 mm due to less dense cone packing	(Hendrickson & Yuodelis, 1984; Provis et al., 2013)
	3 years	0.49 mm, decreasing to 0.35 by 9 years as cones increase density	(Hendrickson et al., 2012)
	Adult	0.35 mm anatomically, though optically magnified on retinal images	(Bringmann et al., 2018)
Foveal pit depth by age	Newborns	Approximately 50-100 µm	(Hendrickson & Yuodelis, 1984)
	1 year	100-140 µm	
	6 years	140-160 µm	(Wagner-Schuman et al., 2011)
	Adult	160-200 µm	(Bringmann et al., 2018)
Sex differences	–	Foveal pit diameter larger in males than in females when adjusted for magnification	(Wagner-Schuman et al., 2011)
	–	No sex differences found in foveal pit shape	

Ethnic variations	–	African children reach mature foveal shape by 15 years	(Wagner-Schuman et al., 2011)
	–	Chinese children reach mature foveal shape by 4 years	(Dubis et al., 2012)
	–	Caucasians reach mature foveal shape by 9 years old	(Wagner-Schuman et al., 2011)
	–	Caucasian males mature slower than females	
	–	African (Americans) males mature faster than females	

Axial length (AL) increases postnatally. It grows from around 16-17 mm at birth to 24 mm in adults (Larsen, 1971; Tideman et al., 2018). Due to the optical properties of the cornea and lens, the retinal image is magnified relative to the true dimensions of retinal structures. Therefore, retinal magnification factors need to be calculated. One commonly employed model is the four-surface Gullstrand schematic eye, which represents the major refractive surfaces of the eye - the cornea, aqueous humor, lens, and vitreous humor (Wang et al., 2019).

The Gullstrand model uses four curved surfaces to represent the refractive interfaces in the eye: the front and back surfaces of the cornea and the front and back surfaces of the lens. Each surface has an associated radius of curvature and refractive index. Together, these optical parameters determine how light is focused. In the study by Wang et al. (2019), the Gullstrand eye model was used to calculate retinal magnification factors and convert between visual angles and retinal distances. They observed that the main factor influencing retinal magnification was axial eye length. They calculated subject-specific retinal magnification factors and estimated the location of the secondary nodal point by adding biometric data from each subject into a Gullstrand model. This made the conversion between the corresponding linear retinal dimensions and visual angle measurements from adaptive optics imaging more reliable.

The fovea's 500 μm central part is a critical eye region characterized by the foveal avascular zone (FAZ), with the highest cone and muller cells presence and an absence of rod photoreceptors (Dubis et al., 2012). The FAZ makes the fovea dependent on blood supply from the choriocapillaris (Hildebrand & Fielder, 2011). FAZ size is relatively consistent but

can range from 0.2mm to 1mm. The shape can also be circular or irregular (Tan et al., 2012). Due to magnification, the FAZ appears larger on retinal imaging; its boundaries can be delineated with fluorescein angiography (Hildebrand & Fielder, 2011).

In the periphery of the retina, we find the ora serrata. The ora serrata serves as a demarcation point, signifying the anterior limits of the sensory retina and the start point of the pars plana region of the ciliary body. At this anatomical juncture, the sensory retina reduces to a monolayer of cells. Anterior to this point, this monolayer transitions into the non-pigmented ciliary epithelium (This is the area where the pigmented ciliary epithelial counterpart supplants the retinal pigment epithelium) (Hildebrand & Fielder, 2011; Kanski, 2015).

Like other components in the neuroretina, the RPE originates in the neuroectodermal embryonic system (Cook et al., 2003). The estimated size of the RPE varies around fourfold, between 14μm in the central retina and 60 μm in the peripheral retina (Boulton & Dayhaw-Barker, 2001). Its density differs according to location; at the fovea, 5,000 cells/m2, and at the periphery, 2,000 cells/m2 (Levin et al., 2011). The pigmentation of the RPE is a rapid process that begins at around 35 days gestation and is complete within approximately one week.

On the other hand, the pigmentation of choroidal melanocytes does not start until the fifth month of fetal life and continues postnatally (Hildebrand & Fielder, 2011). Another pigment lipofuscin, is another pigment produced by the natural degradation of the outer photoreceptor segment in the RPE and Bruch’s membrane (Hildebrand & Fielder, 2011; Kanski, 2015). Lipofuscin levels are a pigment of aging; therefore, we do not find high levels in the retinal pigmented epithelium in children (Marmor, 1999).

Retina layers

The innermost layer of the entire retinal structure is the Inner Limiting Membrane (ILM), formed by the endfeet of Müller cells. Its thickness is within a range of 0.25-2 μm. The ILM is the site for vitreomacular adhesion at the vitreoretinal junction and plays a supporting role in maintaining the overall retinal structure and barrier function (Bonnin et al., 2015; Levin et al., 2011).

The Nerve Fiber Layer (NFL) comprises ganglion cell axons that course toward the optic disc. The thickness of the NFL varies, ranging from 40-150 μm near the optic disc and thinning to 5-15 μm at the macula (Radius & Anderson, 1979). It's worth noting that this thickness can vary among individuals and may be influenced by factors such as age and ocular health (Cook et al., 2003; Hildebrand & Fielder, 2011). The NFL is critical for

transmitting visual signals from the ganglion cells to the brain and is a key parameter often assessed in diagnosing and managing glaucoma (Sommer et al., 1977).

The Ganglion Cell Layer (GCL) houses the nuclei of the ganglion cells and some displaced amacrine cells (Hildebrand & Fielder, 2011). The layer is thickest at the macula, with 1-2 cell layers, and becomes a single-cell layer in the periphery (Levin et al., 2011). These ganglion cells are responsible for transmitting visual signals from the bipolar cells to the brain. Studies on disorders including glaucoma and macular degeneration, where ganglion cell loss is a major concern, are also focused on the GCL (Lee & Yu, 2015; Ventura et al., 2006).

The Inner Plexiform Layer (IPL) contains synapses between bipolar, amacrine, and ganglion cells. The IPL is consistently 30-40 µm thick throughout the retina and plays a significant role in signal processing before transmission to the ganglion cells. The IPL is divided into two main sublaminae: the ON sublamina and the OFF sublamina (Hoshi et al., 2009).

The Inner Nuclear Layer (INL) consists of the cell bodies of horizontal, bipolar, amacrine, and Müller cells (Hildebrand & Fielder, 2011). The INL is thickest at the fovea, with 10-12 cell layers, and progressively thins toward the periphery. Bipolar cells in the INL are crucial for transmitting signals from the photoreceptors to the ganglion cells, while amacrine cells provide modulatory input (Ogden, 1983).

The Outer Plexiform Layer (OPL) is where photoreceptors synapse with bipolar and horizontal cells. The layer is 18-24 µm thick and enables substantial signal processing before transmission to the inner retina (Reynolds & Olitsky, 2010).

The Outer Nuclear Layer (ONL) contains the cell bodies of rod and cone photoreceptors (Wurtz et al., 2000). The ONL is thickest at the fovea, with 10-12 cell layers, and becomes progressively thinner toward the retinal periphery (Levin et al., 2011). Photoreceptors in the ONL perform phototransduction to convert light into electrical signals (Abràmoff et al., 2013). The ONL is particularly vulnerable in diseases like retinitis pigmentosa, where photoreceptor loss is a primary symptom (Menghini et al., 2015).

The External Limiting Membrane (ELM) is not a true membrane but comprises adherens junctions between Müller cells and photoreceptors (Hildebrand & Fielder, 2011). It is crucial for maintaining photoreceptor alignment and overall retinal structure (Kanski, 2015). Its integrity is often assessed in retinal diseases like macular holes (Landa et al., 2012).

As discussed previously (chapter introduction, page 9), the RPE is a cuboidal epithelial monolayer forming the outer blood-retinal barrier (Boulton & Dayhaw-Barker, 2001; Marmor,

1999). The RPE is critical for daily phagocytosis of photoreceptor outer segments and visual pigment recycling (Marmor, 1999). Dysfunction in the RPE is often implicated in diseases like age-related macular degeneration (Boulton & Dayhaw-Barker, 2001).

Bruch's Membrane is an elastic membrane that separates the choriocapillaris from the RPE (Hildebrand & Fielder, 2011). It consists of five layers and varies in thickness between 2-4 μm at the posterior pole and 1-2 μm at the ora serrata (Levin et al., 2011). With age, the membrane thickens, and this thickening is often implicated in the pathogenesis of age-related macular degeneration (Killingsworth et al., 1990).

Optical Coherence Tomography (OCT)

The basic principles of low-coherence interferometry provide the basis for optical coherence tomography (OCT) (Schmitt, 1999). This method involves projecting a low-coherence, high-bandwidth laser beam to the target tissue. A reference beam first split off from the original light source is combined with this light after it scatters and reflects back (Brezinski, 2006). An axial A-scan, which describes the tissue's scattering characteristics along the laser beam path, is created from the interference patterns produced by this technique.

A sequence of A-scans is created when the laser beam is linearly methodically moved over the tissue surface, with each scan representing a distinct point of incidence on the tissue (Wilkinson et al., 2017). The two-dimensional cross-sectional image created by combining these A-scans is known as a B-scan. A detailed three-dimensional representation of the target tissue can be combined by doing B-scans at multiple nearby contiguous areas while following a raster scanning pattern (Brezinski, 2006; Wilkinson et al., 2017).

Concerning image resolution and scanning speed, Optical Coherence Tomography technology has made enormous improvements. The first version, Time Domain OCT (TD-OCT), used a single photon detector and needed a movable mirror to change the reference beam's optical path. This technique could only scan a few thousand A-scans per second (Wilkinson et al., 2017).

A more modern method, called Spectral Domain OCT (SD-OCT), Fourier Domain OCT (FD-OCT), or High-Definition OCT (HD-OCT), makes use of several detectors to record an entire A-scan. As a result, scanning speeds can be increased to over 100,000 A-scans per second, which is almost 200 times faster than TD-OCT (Wylegala, 2011). This also eliminates the requirement for a moving mirror and several reference beams. Scanning speeds for commercial SD-OCT systems typically range from 27,000 to 70,000 A-scans per second (Wilkinson et al., 2017).

This study used the Spectralis OCT-EDI 2 (Heidelberg Engineering, Heidelberg, Germany). The OCT is an SD-OCT device that has become a widely used imaging modality for retinal diseases in multiple investigations. The Spectralis uses a scanning laser ophthalmoscope (SLO) device that allows for simultaneous OCT scans guided by an infrared image of the fundus. This proprietary feature, known as TruTrack Active Eye Tracking, enhances image quality by reducing motion artifacts (*SPECTRALIS OCT - The Modular Imaging Platform | Heidelberg Engineering*, n.d.). The Spectralis OCT-EDI 2 improves upon previous Spectralis models with faster acquisition speeds, improved depth resolution, and an extended scan field of view (Albert et al., 2018).

Several studies have demonstrated the ability of the Spectralis OCT to visualize fine retinal structures, including each of the distinctive layers, the foveal pit, and subtle pathologic changes associated with various retinal diseases (Kiernan et al., 2010). In particular, the high-resolution scans obtained by the Spectralis facilitate detailed morphometric analysis of the fovea (Tick et al., 2011). Measurements of foveal shape, width, and depth can be quantified reliably.

As mentioned previously, the OCT has become the preferred diagnostic tool for evaluating foveal structure, shape, development, and retinal diseases in pediatrics (Vajzovic et al., 2012). Using OCT helps us understand changes in the retina caused by different diseases and evaluate foveal structural variants within the average population (Scheibe et al., 2013). As described previously (chapter introduction, page 10), OCT provides comprehensive structural data to quantify retinal thickness and layer placement. To take advantage of this information, it is critical to consider the location, shape, and reflectivity correlation of the retinal layers. Table 2 gives a structured way that helps analyze the reflectivity correlation.

Table 2. OCT reflectivity correlation of the retinal layers
Source: (Wilkinson et al., 2017)

Structure/Layer	Reflectivity	Location/Additional features
Inner Limiting Membrane	Hyper Reflective	At the vitreoretinal interface
Retinal Nerve Fiber Layer	Hyper Reflective	Within the retina
Plexiform Layers	Hyper Reflective	
Nuclear Layers	Hyper Reflective	
External Limiting Membrane	Hyper Reflective	Not a true membrane but comprises adherens junctions between Müller cells and photoreceptors
Retinal Vessels	Hyper Reflective	Circular structures in the inner retina; vertical shadows extend into deeper layers.

Relationship between foveal width and depth

As described above, the relationship between foveal width and depth is complex, and different factors such as age, sex, and even ethnicity can influence each measurement independently. For example, a deeper fovea suggests thicker foveal tissue (or absence of foveal bulge); it can also be a sign of foveal detachment or macular edema, both of which can have an impact on the visual acuity (Iannetti et al., 2023). Therefore, it is crucial to have a robust set of normative data that accounts for these variables. This is particularly important in pediatric populations, where early diagnosis of abnormal development can have long-term implications for visual health (Hendrickson et al., 2012). Understanding how the fovea changes with age is essential to help us develop tools for early detection of abnormal changes (Dubis et al., 2012). Its size, shape, and position can vary among subjects, and its dimensions are essential indicators of retinal health (Sasaki et al., 2022). Another diagnostic indicator is the thickness of the retinal layers, especially the outer layers. Clinicians can diagnose abnormal development early on due to variations in retinal thickness (Hendrickson et al., 2012).

Pathologies and disorders

Different studies have evaluated retinal thickness associated with various eye diseases and disorders. Still, a limited number of studies have evaluated retinal thickness in normal healthy eyes. The introduction of OCT imaging has facilitated the evaluation of eye disorders or diseases.

Retinopathy of prematurity (ROP) is a vasoproliferative disease in premature infants that can lead to retinal detachment and blindness (Chang, 2019). OCT allows detailed evaluation of structural changes in ROP, including intraretinal cysts, subretinal fluid, retinoschisis, and disruption of the photoreceptor layers (Anwar et al., 2023). OCT also helps with diagnosing and monitoring the progression of inherited retinal dystrophies like Leber congenital amaurosis, achromatopsia, and Stargardt disease through the detection of ellipsoid zone disruption, retinal thinning, and other characteristic morphologic abnormalities. For example, in patients with Leber congenital amaurosis diseases, the OCT analysis revealed retinal dystrophies, reduced macular thickness, and RPE lesions (Testa et al., 2011). Additionally, OCT has become integral to the assessment of Best disease, coats disease, familial exudative vitreoretinopathy (FEVR), pediatric melanoma, retinoblastoma, degenerative myopia, and numerous other pediatric retinal conditions (El-Dairi et al., 2009; Finn et al., 2019; Seresirikachorn et al., 2023). The ability to perform precise quantitative measurements and detailed mapping of pathologic changes longitudinally has improved the diagnosis and monitoring of pediatric retinal diseases. Details given in Table 3 summarize some of the pediatric population's most common diseases and disorders and their respective OCT findings.

Table 3 Most common diseases and disorders in children

Source: (Anwar et al., 2023; Chang, 2019; Cook et al., 2003; El-Dairi et al., 2009; Finn et al., 2019; Hildebrand & Fielder, 2011; Raynor et al., 2021)

Disease/Disorder	OCT Findings
Best Disease	Detailed visualization of vitelliform lesions as highly reflective dome-shaped accumulations under the neurosensory retina. Atrophic changes in advanced stages, with the disappearance of the photoreceptor layers.
Coats Disease	Telangiectatic retinal vessels and aneurysms. Subretinal fluid, retinal thickening and detachment, cystoid macular edema, and subfoveal deposition of exudates.
FEVR	Folding and distortion of inner retinal layers. Exudative retinal detachments and cystic retinal degeneration. Macular dragging and traction.
Pediatric Melanoma	Subretinal fluid, retinal thickening, and outer retinal irregularities
Retinoblastoma	Dome-shaped tumor mass with moderate-to-high internal reflectivity Optical shadowing posterior to mass. Common detachment of retina overlying the tumor.
Degenerative/High Myopia	Posterior staphyloma, chorioretinal atrophy, lacquer cracks, myopic foveoschisis, and macular atrophy.
ROP	Prominent, jagged vasoproliferation at the vascular and avascular peripheral retina junction. Intraretinal edema, subretinal fluid, fibrovascular proliferation, vitreoretinal traction, and retinal detachment in advanced cases

Sex and ethnicity

We have learned that retinal thickness significantly varies among different ages, sexes, and ethnic groups (Kelty et al., 2008; Wagner-Schuman et al., 2011; Won et al., 2016). Ethnicity has been found to play a significant role in foveal thickness, with the African race having significantly thinner retinas than Caucasians (Asefzadeh et al., 2007). Chinese children have been found to exhibit specific patterns of macular and peripapillary retinal nerve fiber layer thickness (Lee et al., 2015). Studies in the United States have shown a significant difference in foveal thickness between males and females. However, further investigation is required to determine if a significant difference exists between more extensive ethnic groups (Barak et

al., 2011). Understanding these ethnic, sex, and age-specific variations is crucial for accurate diagnosis and understanding of the human eye's normal development.

Importance of this study

Previous studies have analyzed the fovea's shape and compared it in the adult population (Mirhajianmoghadam et al., 2020). Changes in children's fovea have not been well documented, especially in Nordic children. The study by Dubis et al., 2009 shows no significant differences in diameter, depth, and slope of the fovea pit between subjects aged 13 and 52. This study was not limited to the Nordic population. This current gap in the information of the Nordic population about the fovea's shape makes this study necessary.

Limitations

One of the principal limitations of this study was the small sample size (n=78) from a homogeneous Norwegian population. The findings require validation in a larger cohort. In particular, the lack of axial length difference between age groups indicates further investigation with bigger samples.

Additional limitations include the narrow age range examined. Foveal development likely undergoes earlier dynamic changes in the first years of life (Dubis et al., 2012). Future research should focus on younger ages to understand the earliest development processes.

Additional anterior segment dimensions could have tested a more complex investigation of the effects of optical magnification. Optical magnification from the cornea and lens on OCT imaging makes the retinal structures seem larger than their actual anatomical sizes (Bennett et al., 1994; Yuodelis & Hendrickson, 1986). Other measurements could be used to account for magnification to quantify actual foveal morphology. For example, anterior chamber depth (ACD) influences magnification and axial length (Bennett et al., 1994). Deeper anterior chambers increase retinal magnification.

Some studies suggest ACD exhibits a developmental trajectory distinct from axial elongation in childhood (Bengtsson & Krakau, 1992; Garway-Heath et al., 1998; Ojaimi et al., 2005). Measuring ACD would allow the calculation of an alternative magnification adjustment factor using optical modeling formulas (Bennett et al., 1994; Wu et al., 2018). This could improve the estimation of true anatomical foveal width and depth.

Furthermore, corneal power and curvature affect image scaling. Detailed keratometry data combined with ACD and axial length could enable better optical models using ray-tracing software like Zemax (Wu et al., 2018). This study was limited in accounting for magnification

effects by only measuring axial length. This could be implemented in future studies to see if there is a significant difference with the magnification correction used in this master thesis.

It is essential to consider additional variables like genetics, environmental influences, and lifestyle factors that may affect the foveal shape, axial length, and other ocular growth metrics. The complex interplay between anatomical characteristics should be analyzed in future studies.

2 Purpose and research questions

The aim of this study is to conduct a comprehensive assessment of foveal morphology and outer retinal layer thickness in a cohort of Norwegian children aged 7-8 and 10-11. By analyzing segmented images from the Spectralis optical coherence tomography (OCT) and biometrical data, the study aims to statistically give results of normative data on the pediatric Norwegian population.

The study's objectives are divided into four categories:

Normative Data: To establish normative data for foveal shape and outer retinal layer thickness in a group of Norwegian children, which can serve as a reference for diagnosing and managing retinal pathologies.

Sex Differences: To investigate whether there are any sex-based differences in foveal shape and outer retinal layer thickness, which could have implications for understanding sex-specific risks for certain ocular conditions.

Developmental Changes: To examine how the fovea and outer retinal layer differ between the ages of 7-8 and 10-11, providing information on the maturation process of the retina during this period of visual development.

Ethnic Specificity: To control for potential ethnic influences by focusing on a homogeneous Norwegian cohort, thereby enhancing the specificity and applicability of the findings to the Norwegian population in the local clinical practice.

Research Questions

To achieve the previous objectives, the study is guided by the following research questions:

Foveal Shape in Males vs. Females: Is there a statistically significant difference in the foveal shape between males and females who grew up in Norway?

Hypothesis: There is a measurable difference in foveal shape parameters, such as foveal width, depth, and slope, between males and females.

Outer Retinal Layer Thickness in Males vs. Females: Is there a statistically significant difference in the outer retinal layer thickness at the fovea between males and females who grew up in Norway?

Hypothesis: There is a measurable difference in the thickness of the outer retinal layers between males and females.

Age-Related Changes in Foveal Shape and Outer Retinal Layer Thickness: Do the foveal shape and outer retinal layer thickness at the fovea change significantly from ages 7-8 to 10-11 in children who grew up in Norway?

Hypothesis: There are developmental changes in foveal shape and outer retinal layer thickness between the two age groups, reflecting the ongoing maturation of the retina.

Significance of the Study

The results of this study will not only fill a gap in the existing literature but also provide the groundwork for future research. Understanding children's normal developmental patterns of the fovea and outer retinal layers is crucial for distinguishing pathological changes from normal variations. Consequently, this will simplify identifying and treating different retinal diseases at an early stage, improving the quality of life for those afflicted.

By addressing these research questions, the study aims to contribute significantly to pediatric optometry, particularly in the context of the Norwegian population.

3 Methods

Design

This study used a cross-sectional design to compare foveal morphology between two age groups of healthy Norwegian children. Cross-sectional studies measure outcomes in different population groups at a specific point in time. This enables comparisons of outcome differences between groups, such as age-related developmental changes (Carlson & Morrison, 2009).

The cross-sectional design is appropriate to address the research questions investigating if the foveal shape and outer retinal layer thickness differ between age groups and sexes in childhood. Cross-sectional studies can efficiently assess multiple outcomes in defined cohorts simultaneously. They can effectively estimate outcome prevalence and quantify group differences (Mann, 2003).

Two different age groups of young school-aged children were recruited. Retinal imaging and eye exams were performed to extract quantitative foveal parameters for statistical comparisons. This cross-sectional approach provided information on the normal data of childhood foveal development in a Norwegian population.

Settings and participants

The study population comprises children between 7 and 11 who grew up in Norway. The total number of subjects is 78, with an equal distribution of 50% males and 50% females (Figure 1). The children aged 7-8 group includes 41 children (21 males and 20 females), while the children aged 10-11 comprise 37 children (18 males and 19 females).

The inclusion criteria were age between 7-11 years, normal ocular health with no history of retinal disease, and stable fixation ability. Children with developmental disorders were excluded.

Figure 1 Study population distribution

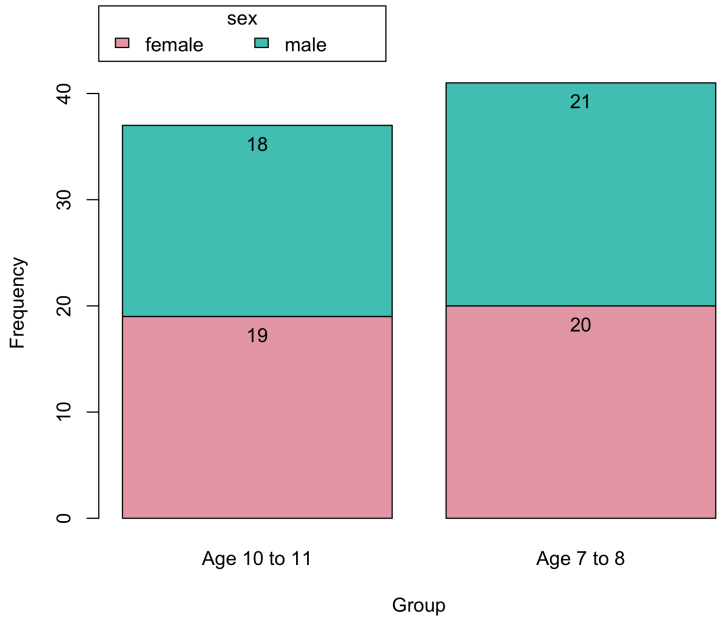

Data collection

OCT images, ocular biometry, and cycloplegic autorefraction measures included for analysis were obtained from the USN Colour Vision and Retinal Imaging Laboratory database. All OCT images were acquired with the Spectralis OCT-EDI 2 (Heidelberg Engineering, Heidelberg, Germany). Ocular biometry measures were obtained with IOLMaster 700 (Carl Zeiss Meditec AG, Jena, Germany) while cycloplegic autorefractor was obtained with HRK-8000A (Huvitz Co., Ltd., Gyeonggi-do, Korea) 20 minutes after instillation of topical 1% cyclopentolate hydrochloride (Minims single-use; Bausch + Lomb UK Ltd, Kingston upon Thames, UK).

Segmentation

Every OCT scan is segmented using custom software developed by the CVRI research group “Kongsberg OCT Segmentation and Analysis” (Version: 1.4.187 gffdaf48, 2022-11-27).

The segmentation of the layers begins with a semiautomatic active contour method, which detects the anterior edge of the inner limiting membrane (ILM) and the posterior boundary of the retinal pigmented epithelium-Bruch’s membrane (RPE-BrM) of the central foveal OCT scan (Baraas et al., 2022). The active contour method helps smooth the segmented contours and allows the operator to correct any segmentation error, like image artifacts and noise. The area to analyze in the fovea will be the section with maximum photoreceptors located at the fovea center (Pedersen et al., 2020).

Each layer segmentation is done after scaling the layers of the scan; this is done to account for individual differences in retinal magnification and ensure a valid measurement of the thickness of the retinal layers. The lateral scales of all the OCT scans were scaled for each participant's respective individual retinal magnification ratio using the Gullstrand four-surface schematic eye model (Wang et al., 2019). A successful measurement of the foveal zone is considered when finding the center of the fovea in each image.

The segmentation of retinal layers from OCT B-scans used active contour " snake" (an artificial neural network approach for identifying image contours). The snake algorithm implements deformable models that minimize an energy function based on internal constraints like smoothness and external image features like edges. This enables semi-automated segmentation by balancing automated contour detection with interactive refinement. This information is in the software's user guide, and according to it, the use of the snake has been used successfully in other studies (Mishra et al., 2009).

For each OCT B-scan, the ILM layer was first segmented by initializing the snake and adjusting the control points until the contour aligned with the layer boundary. The algorithm automatically segmented the nerve fiber layer (NFL), ganglion cell layer (GCL), inner plexiform layer (IPL), and inner nuclear layer (INL) layers to reach the outer plexiform layer (OPL) layer of interest. Careful manual snake adjustment was performed to identify the OPL boundary accurately. Once satisfied with the OPL segmentation, earlier NFL, GCL, IPL, and INL segmentations were deleted as they were not required for this study. The algorithm then segmented the ELM and RPE layers to complete the relevant layer boundaries.

The interactive snake refinement was critical for accurate segmentation, as artifacts and noise can mislead fully automated approaches. The resulting segmented layers enabled precise thickness measurement of the retinal layers involved in foveal development. The software outputs foveal depth, width, and ONL thickness measurements calculated from the segmented ILM, OPL, ELM, and RPE layers (Figure 2). Thus, the snake algorithm balanced efficiency and accuracy by combining automated contour detection with manual adjustment to overcome the limitations of fully automated segmentation. The meticulous interactive refinement ensured robust retinal layer segmentation to quantify foveal parameters precisely.

Figure 2 Semiautomatic segmentation image

Source: Kongsberg OCT Segmentation and Analysis software

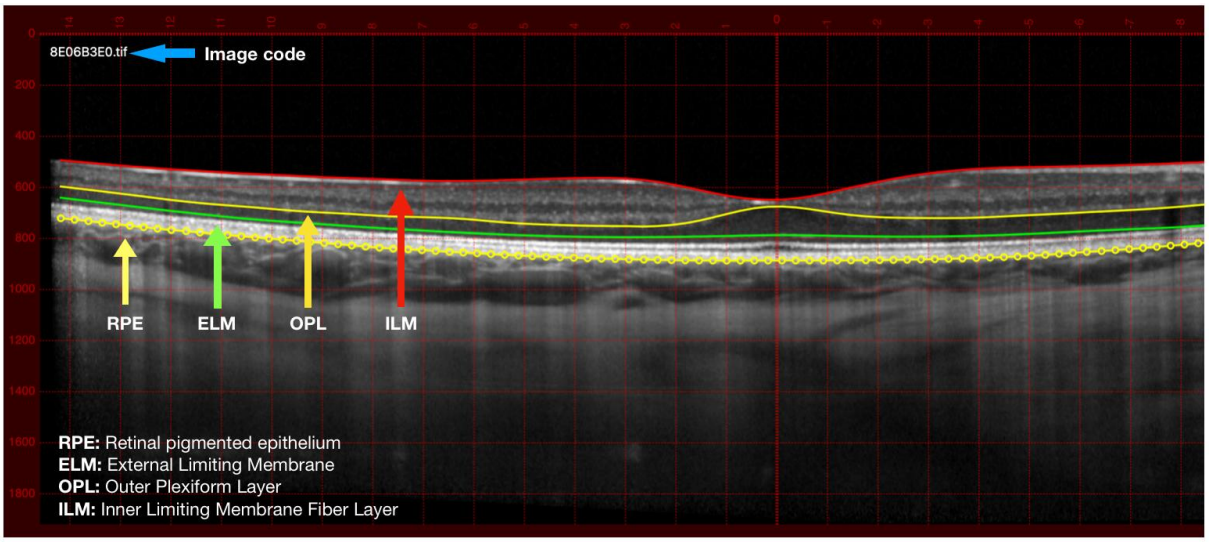

Definition of variables in extracted data collection

- Spectralis date of test: Time stamp used by the Spectralis OCT of the actual B-scan
- Series ID: Identification number of the B-scan.
- Fovea parameters are given in microns (µm). Figure 3
    - Fovea width: Defined as the lateral distance between nasal and temporal peak macular thickness. The peak macular thickness is placed on an A-scan on either side of the fovea, where the distance between the internal limiting membrane (ILM) and the retinal pigment epithelium (RPE) is highest. This measurement is in pixels but multiplied by the lateral microns-per-pixel scaling, as determined from the corresponding IOLMaster measurement and the Gullstrand 4-surface model.
    - Fovea depth: Defined as the sum of the nasal and temporal peak macular thickness A-scans, divided by two (subtracting the ILM and RPE thickness at the fovea).
    - Outer Nuclear Layer (ONL) at the fovea: Defined as the distance in an A-Scan between the outer plexiform layer (OPL) and the external limiting membrane (ELM).

Figure 3 Fovea parameters

Source: (Tick et al., 2011)

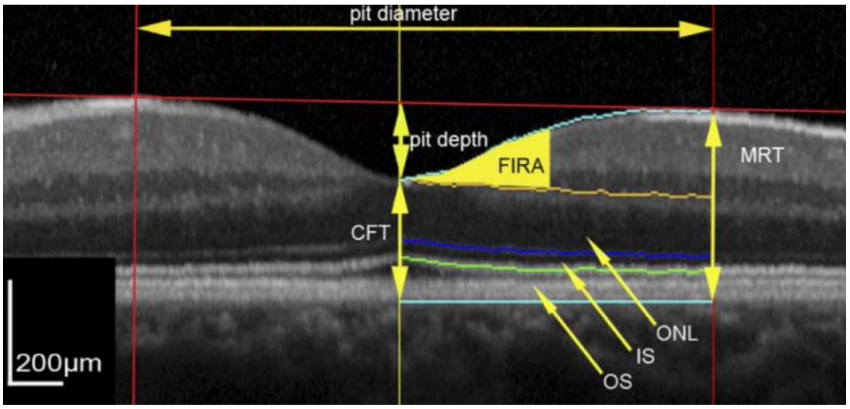

- Eye axial length (AL): This measurement is given millimeters (mm).

- Corneal radius (CR) refers to the curvature of the cornea in millimeters (mm) (maximal or steepest radius R1 + minimal or flattest radius R2 / 2.0) of the tested eye. The relationship between SER and CR is essential in determining the appropriate prescription for corrective lenses, such as glasses or contact lenses, to achieve optimal visual acuity.

- Cyclo: True or false. Determines whether the measurement was taken during cycloplegia or not.

- Spherical Equivalent Refraction (SER): Measurement of the total refractive error of the eye, taking into account both the spherical and cylindrical components (sphere + 0.5*cylinder), and is expressed in diopters (D).

Analysis

Statistical analysis

The statistical analysis in this study is made with R Version 2.8-0 (R Foundation for Statistical Computing, Vienna, Austria).

R Commander is a basic statistics graphical user interface (GUI) created by the R Foundation for Statistical Computing. As an open-source platform, R Commander provides a powerful and user-friendly tool for the statistical analysis of various data types.

The features of R Commander make it a good choice for studying pediatric foveal data. First, the GUI format allows users without coding experience to access R's wide range of statistical tests and graphics. Options include summary statistics, regression models, ANOVA, contingency tables, and many common parametric and nonparametric tests. Plots like histograms, box plots, and scatter plots can be generated. Because of its simplicity, researchers and clinicians can apply robust statistical methods to ophthalmologic data. Second, R Commander is a free, open-source, customizable, platform-independent, user-friendly GUI for R that provides cost-effective access to advanced statistics for underfunded research through its large support community and extensibility.

R Commander has various kinds of statistical analyses. To provide a comprehensive overview of the functionalities that are used in this master thesis, here is a short description (Fox, 2016):

Descriptive Statistics

Descriptive statistics are foundational elements in statistical analysis. They summarize and describe the key features of a data set by providing its main characteristics. For this study, these were used:

- Mean: The arithmetic average of a set of values.
- Median: The middle value that separates the data set into two equal halves.
- Mode: The most frequently occurring value in a data set.
- Standard Deviation: A measure of the dispersion of a data set from its mean.
- Variance: The average of the squared differences from the mean.

These statistics are fundamental in optometric research.

Inferential Statistics

Inferential statistics enable researchers and clinicians to make conclusions about a specific population based on a sample.

Various parametric and non-parametric hypothesis testing tools are available through R Commander.

Parametric tests make certain assumptions about the parameters of the population distribution from which the samples are drawn (Van Buren & Herring, 2020). The most common assumptions are that the data are normally distributed, samples are drawn independently, and variances are equal across groups.

Commonly Used Parametric Tests in R Commander

- T-tests: Utilized for comparing the means of two groups. A one-sample t-test can assess whether a sample mean significantly differs from a known or hypothesized value. An independent sample t-test can evaluate the equality of means between two separate groups. In contrast, a paired t-test compares the means of the same group before and after treatment (Fox, 2016).
- Analysis of Variance (ANOVA): ANOVA is the preferred method when there are more than two groups to compare. One-way ANOVA assesses whether there are statistically significant differences between the means of three or more independent groups. Two-way ANOVA allows for examining the effects of two independent variables on a dependent variable (Fagerland, 2012; Fox, 2016).

Non-parametric tests do not make as many assumptions about the population distribution and are thus more robust against violations of these assumptions. They are often used when the data is skewed, ordinal, or not measured in a way that allows for a normal distribution to be assumed (Van Buren & Herring, 2020).

Commonly Used Non-Parametric Tests in R Commander

- Two-Sample Wilconxon test: This test is designed to compare two independent samples to determine if they come from populations with identical distribution shapes. It is less stringent in its assumptions than the t-test, making no assumptions about the data distribution.
- Single-Sample Wilconxon test: The single-sample Wilcoxon test, often called the Wilcoxon signed-rank test, compares the median of a single sample to a specific value.
- Paired-Samples Wilconxon test: This test compares two sets of related scores, observations, or measurements to assess whether their population mean ranks differ.
- Krusdal-Wallis test: It is equivalent to the one-way ANOVA and is used when comparing more than two independent groups.
- Friedman Rank-Sum test: It is used for repeated measures and ranks the data to compare medians across different conditions (Fox, 2016).

Regression Analysis

Regression analysis investigates the relationship between a dependent variable and one or more independent variables. This is important for predicting outcomes and understanding underlying correlations.

- Linear Regression: Estimates the relationship between two numerical variables.
- Multiple Regression: Estimates the relationship between multiple independent variables and a dependent variable.

Normality Tests

Checking whether your data follows a normal distribution is necessary before using specific statistical tests. R Commander offers options for performing normality tests like:

- Shapiro-Wilk: A widely used method for testing normality.
- Anderson-Darling: A modification of the Shapiro-Wilk test that gives more weight to the tails.

Using this test and the visualization of the data in a histogram helps us determine whether the data is normally distributed or not.

Data Visualization

Exploratory data analysis primarily depends on visualizations of information to help identify patterns, trends, and abnormalities in large data sets. R Commander has the following alternatives:

- Scatter Plots: For visualizing relationships between two numerical variables.
- Box Plots: For visualizing the central tendency and spread of data.
- Histograms: For visualizing the frequency distribution of a data set.

Understanding the numerous variables and behaviors present in the pediatric population can benefit from each type of plot in a different way.

Data results are written in MEAN ± STANDARD DEVIATION (RANGE). A normality test (Shapiro-Wilk was used) is performed to apply parametric tests in the cases that apply. The data that has no normal behavior is analyzed with non-parametric tests. Every statistical parametric and non-parametric test has a confidence level of 0.95 (P-value < 0.05 was considered significant).

A comma-separated values (CSV) file was used to store the data that was extracted from the OCT's image segmentation. This choice was made because of the fact that CVS files use plain text files with a relatively simple structure, where each line of the text file represents a row of a table, and the individual points are separated by commas to form the columns. Despite the benefits of CSV files, such as their portability, simplicity, and potential for version control tracking, there are a number of subtly incompatible CSV file variations, including several different formats. Different software interprets the dialect of the file, which helps solve this problem (van den Burg et al., 2019).

All quantitative data was stored in CSV format on a secure network drive with access restricted to study personnel through password-protected user accounts. Participant identifiers were anonymized by assigning randomized ID codes. The key linking codes to identifiable information were stored separately from the data files. At study completion, this key will be destroyed to anonymize the data fully.

Validity and Reliability

The Spectralis OCT-EDI 2 system used for retinal imaging has high repeatability for quantifying retinal layer thicknesses compared to histological measures, enhancing validity (according to results in different studies included in the reference section of the current study). All OCT scans were segmented using manual verification to ensure accurate retinal layer boundary delineation for measuring foveal parameters.

Ocular biometry was performed with the ZEISS IOLMaster 700, which has high precision and reproducibility, further improving reliability. The standardized imaging and analysis protocols establish robust, consistent quantification of foveal dimensions and biometry for valid statistical comparisons across groups.

Research Ethics

This study has received approval from the Regional Committee for Medical Research Ethics for the Southern Norway Regional Health Authority (Ref. 2019/578) and SIKT registered (Ref. 618194).

According to the research protocol (Suncin A., 2022), all the participants have already signed an informed consent and were fully explained the study procedures.

Informed Consent

All child participants and their parents/guardians underwent an informed consent process before enrollment. They received detailed written and verbal information about the study objectives, procedures, risks, benefits, privacy protections, and right to withdraw. Signed informed consent was obtained from the parents/guardians.

Confidentiality

To protect confidentiality, participant names and contact details were replaced with randomized ID codes. The key linking IDs to identifiable information was stored securely on a password-protected server separate from the study data. Only the principal investigator and approved personnel had access to the key. The key will be permanently deleted after study completion to anonymize the data.

Data Storage

All images and data collected were stored electronically on a secure server, encrypted and password-protected. Access was restricted to authorized study personnel. At the end of the study, the data will continue to be stored securely for future research purposes.

Right to Withdraw

Participants were informed they could withdraw from the study at any time without providing a reason. If a participant withdrew consent, all associated data would be deleted and only analyzed in anonymized aggregate form. Withdrawing would not affect the child's treatment or care at the university.

Risk-Benefit Assessment

The risks involved were minimal. The retinal imaging was non-invasive, with only a moment of mild discomfort from the camera flash/lights and eye drops. There was no direct benefit to participants. The societal benefits of understanding foveal development in children were accordingly explained to the participants.

4 Results

A total of 78 children were included in this study, divided into two age groups. The group of children between 7 and 8 years old consists of 41 children, with 21 males and 20 females, while the group of children between 10 and 11 years old consists of 37 children, with 18 males and 19 females. All the eyes tested were right eyes (RE). The analysis of all subjects by age group gave the following results: The eye's axial length was measured in millimeters (mm). The overall mean axial length was 22.87 ± 0.73 mm, ranging from 21.24 to 24.54 mm. A comparative analysis between the two age groups showed no statistically significant difference (p=0.2268). The fovea width was measured in micrometers (µm); it had an overall mean of 2283.78 ± 203.17 µm, with a range of 1682 to 2727 µm. Again, no significant difference was observed between the age groups (p=0.9172). The fovea depth was also measured in micrometers, with an overall mean of 123.49 ± 19.64 µm and a range of 70 to 166 µm. No significant age-related difference was noted (p=0.1958). The ONL thickness at the fovea was 98.44 ± 9.93 µm, ranging from 74 to 127 µm. Statistical analysis revealed no significant difference between the age groups (p=0.7011). The mean corneal radius (CR) was 7.79 ± 0.26 mm, ranging from 7.26 to 8.45 mm. No significant age-related difference was observed (p=0.4696). The Spherical Equivalent Refraction (SER) was measured in diopters, with a mean value of 1.24 ± 0.93 D, ranging from -1.14 to 5.67 D. No significant difference was observed between the age groups (p=0.1865).

Table 4. Summary of the descriptive statistics of all study subjects by age group.

	All subjects	Age 7 to 8 years old	Age 10 to 11 years old	p-value
Number of eyes	78	41	37	-
Sex (male/female)	39/39	21 males / 20 females	18 males / 19 females	-
Axial length (mm)	22,87 ± 0,73 (21,24 to 24,54)	22,78 ± 0,67 (21,63 to 24,35)	22,98 ± 0,78 (21,24 to 24,54)	0,2268
Fovea width (µm)	2283,78 ± 203,17 (1682 to 2727)	2281,46 ± 183,46 (1682 to 2609)	2286,35 ± 225,56 (1829 to 2727)	0,9172
Fovea depth (µm)	123,49 ± 19,64 (70 to 166)	120,76 ± 20,43 (70 to 166)	126,51 ± 18,53 (93 to 166)	0,1958
Outer Nuclear Layer (ONL) thickness at fovea (µm)	98,44 ± 9,93 (74 to 127)	98,02 ± 10,53 (74 to 127)	98,89 ± 9,36 (82 to 121)	0,7011

CR (mm)	7,79 ± 0,26 (7,26 to 8,45)	7,81 ± 0,26 (7,40 to 8,45)	7,77 ± 0,25 (7,26 to 8,20)	0,4696
SER (Diopters)	1,24 ± 0,93 (-1,14 to 5,67)	1,38 ± 0,78 (-0,67 to 3,49)	1,09 ± 1,06 (-1,14 to 5,67)	0,1865

Relationship between all subjects divided by sex and foveal shape

The analysis of all subjects by sex gave the following results (See table 5): The mean axial length for females was 22.63 ± 0.53 mm, ranging from 21.63 to 23.90 mm. The mean axial length for males was 23.12 ± 0.82 mm, ranging from 21.24 to 24.54 mm. A statistically significant difference was observed between the sexes with a p=0.003* (See Figure 4). The fovea width for females had a mean of 2303.33 ± 195.5 µm, ranging from 1961 to 2727 µm. For males, the mean was 2264.23 ± 211.28 µm, ranging from 1682 to 2651 µm. No significant gender-based difference was observed (p=0.399). The fovea depth had a mean of 122.97 ± 15.99 µm for females and 124 ± 22.92 µm for males. The range for females was 88 to 166 µm, and for males, it was 70 to 166 µm. No significant difference was noted between the genders (p=0.819). For females, the ONL thickness at the fovea was 99.28 ± 10.29 µm, ranging from 79 to 127 µm. For males, it was 97.59 ± 9.62 µm, ranging from 74 to 122 µm. No significant gender-based difference was observed (p=0.455). The mean corneal radius for females was 7.76 ± 0.24 mm, ranging from 7.26 to 8.20 mm. For males, it was 7.83 ± 0.27 mm, ranging from 7.34 to 8.45 mm. No significant difference was observed (p=0.278). The SER was measured in diopters. For females, the mean SER was 1.31 ± 0.64 D, ranging from 0.30 to 2.65 D. For males, it was 1.18 ± 1.15 D, ranging from -1.14 to 5.67 D. No significant gender-based difference was observed (p=0.553).

Females had a significantly shorter axial length than males (22.63 ± 0.53 mm vs 23.12 ± 0.82 mm, p=0.003). However, there were no significant differences between females and males in foveal width, depth, or ONL thickness (all p>0.05).

Table 5. Summary of the descriptive statistics by sex.

	Females	Males	p-value
Axial length (mm)	22,63 ± 0,53 (21,63 to 23,90)	23,12 ± 0,82 (21,24 to 24,54)	0,003*
Fovea width (µm)	2303,33 ± 195,5 (1961 to 2727)	2264,23 ± 211,28 (1682 to 2651)	0,399
Fovea depth (µm)	122,97 ± 15,99 (88 to 166)	124 ± 22,92 (70 to 166)	0,819
Outer Nuclear Layer (ONL) thickness at fovea (µm)	99,28 ± 10,29 (79 to 127)	97,59 ± 9,62 (74 to 122)	0,455
cr (mm)	7,76 ± 0,24 (7,26 to 8,20	7,83 ± 0,27 (7,34 to 8,45)	0,278
SER (Diopters)	1,31 ± 0,64 (0,30 to 2,65)	1,18 ± 1,15 (-1,14 to 5,67)	0,553

Figure 4. Mean of axial lengths by age group

AL/CR ratio

The ratio AL/CR is the ratio of the eye axial length to the corneal radius. It is a measure of the shape and size of the eye. It is calculated by dividing the eye axial length (AL) by the corneal radius (CR).

The relationship between SER and AL/CR is a variable that helps us determine if there is a hyperopic or myopic tendency (See Figure 5). The AL/CR ratio ranges from 2.738 to 3.153, with a mean of 2.937 and a standard deviation of 0.083.

Figure 5. Scatter-plot between SER and AL/CR plotted by sex

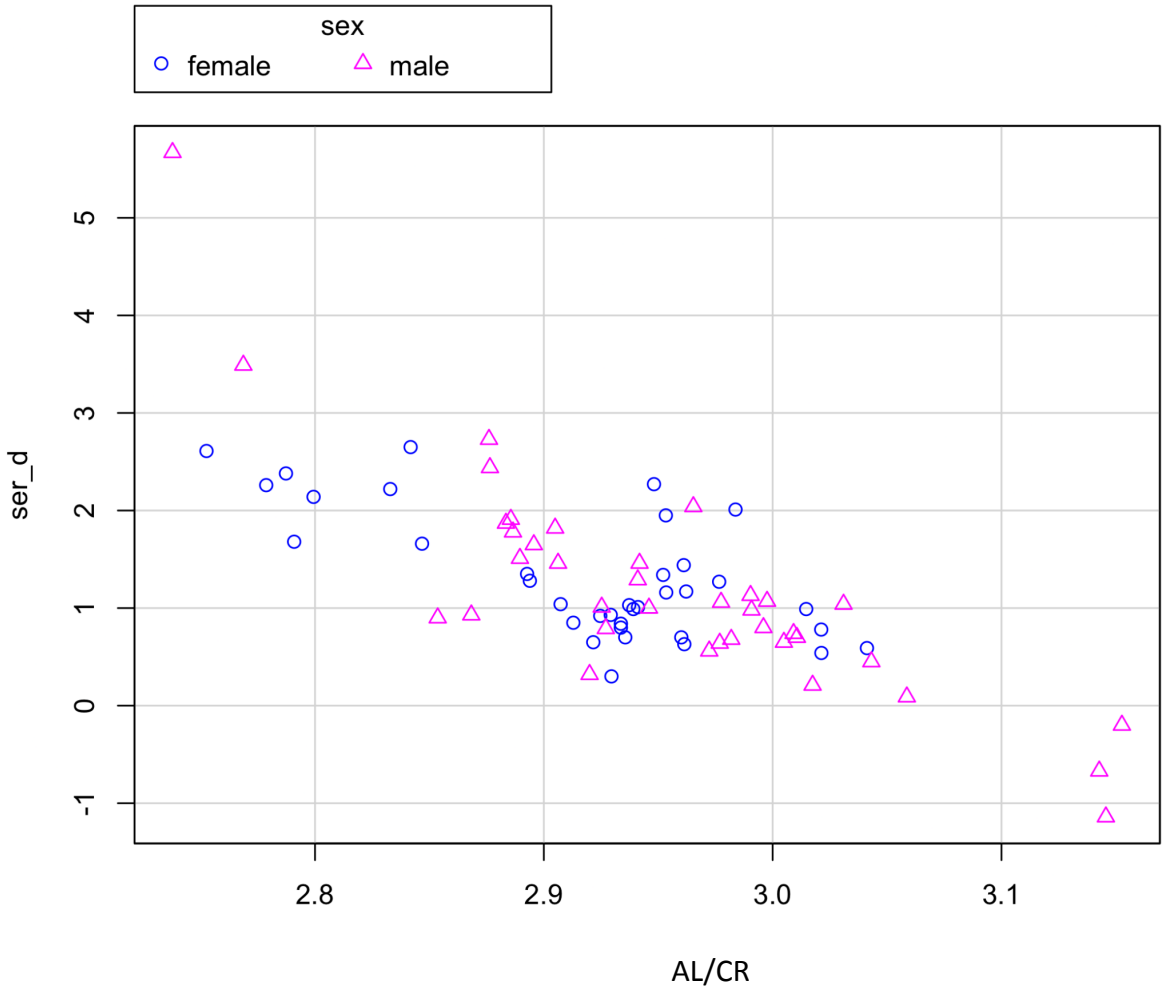

- There is a negative correlation between SER and AL/CR, as expected based on the principles described above. Eyes with higher AL/CR ratios (towards the right) tended to have more negative SER, indicating myopia (Ojaimi et al., 2005; Tideman et al., 2018). Eyes with lower AL/CR ratios (left) had less negative or positive SERs indicating hyperopia.

- Most eyes clustered around 0 to 2 diopters of SER, showing low to moderate hyperopia.

- A few outliers with high hyperopia (SER > +3D) had low AL/CR ratios below 3.0, indicating shorter axial lengths and steeper corneas.

- The females clustered nearer the center with less variability in AL/CR and more hyperopic refractions on average compared to males. Males showed more dispersion and more myopic refractions.

- The distribution and lack of clear age-related patterns suggest variables besides age impact refractive development in this age group. It is probable that both genetic and environmental variables have to be considered.

Figure 6. Changes in the thickness in the foveal depth and width and changes in the ONL thickness at the fovea

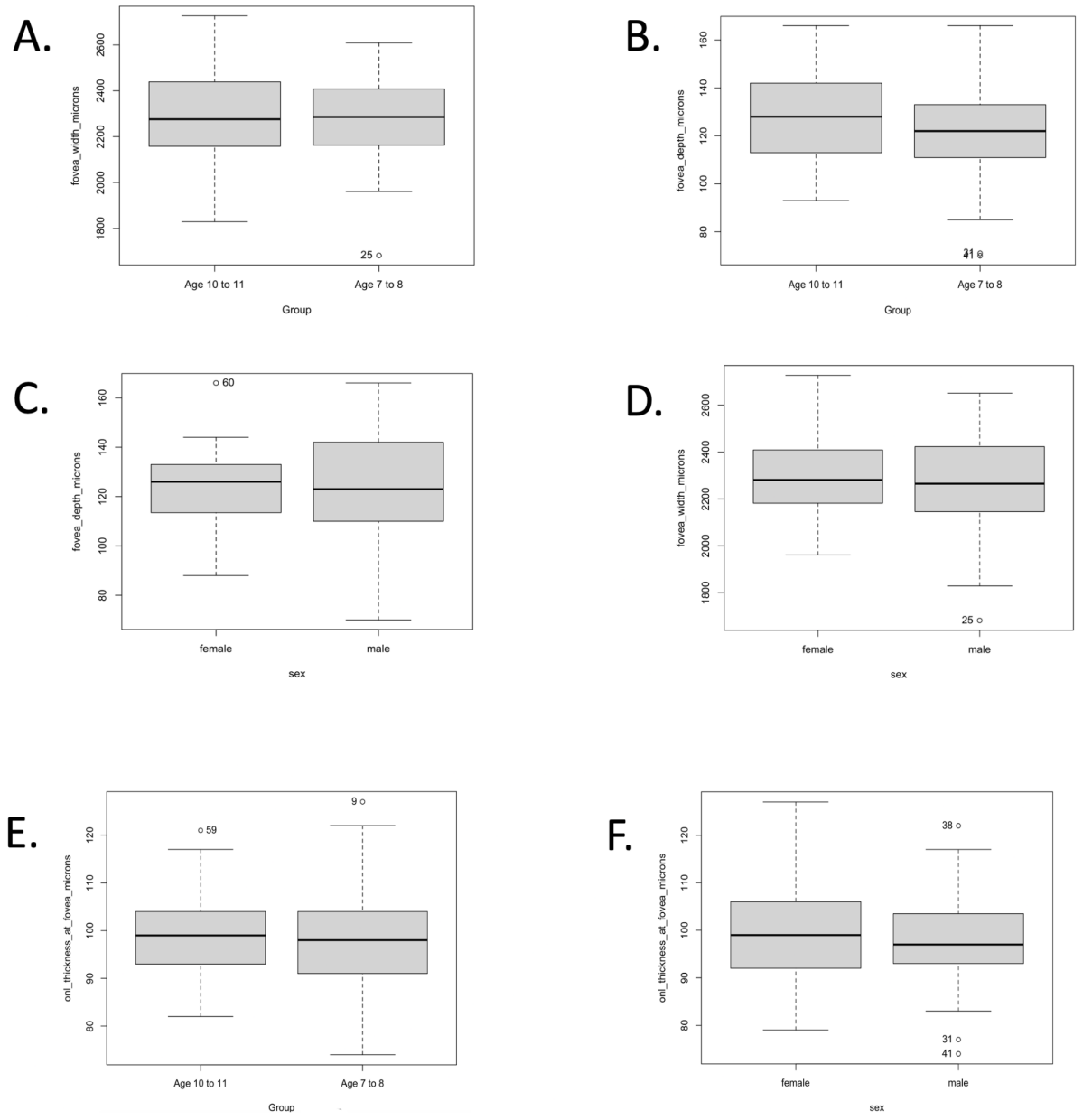

Figure 6 shows the changes in the thickness in the foveal depth (B, C) and width (A, D), as well as changes in the ONL thickness at the fovea (E, F). In females, we observe no significant difference in these values. Foveal width increased from age seven to eleven by 0,92%, the foveal depth increased by 5.58%, and the ONL thickness at the fovea decreased by 0.84%. In the male group, there were also no significant differences in foveal width from age seven to eleven but an increased thickness of 1,58%, foveal depth increased by 8,44%, and ONL thickness at the fovea increased by 2,90%.

The Spearman correlation tests were employed to assess the relationship between foveal shape (both width and depth) and two key ophthalmic metrics: AL and AL/CR (Axial Length to Corneal Radius ratio). The Spearman test is non-parametric, making it robust against non-normal distributions and outliers, thus providing a more conservative correlation measure.

Spearman Correlation Coefficients and P-values

1. Fovea Width vs. AL/CR: p=0.0665
2. Fovea Depth vs. AL/CR: p=0.6569
3. Fovea Width vs. AL: p=0.6852
4. Fovea Depth vs. AL: p=0.4260

Spearman's correlation found no association between foveal width and axial length/corneal radius ratio (rs=0.132, p=0.0665) or axial length (rs=0.043, p=0.6852). There was no correlation between foveal depth and axial length/corneal radius ratio (rs=0.037, p=0.6569) or axial length (rs=-0.102, p=0.4260).

Age-based Comparison (7-8 vs 10-11)

1. Fovea Width vs. AL/CR: p=0.2264
2. Fovea Depth vs. AL/CR: p=0.2078

Gender-based Comparison

Fovea Width vs. AL/CR: p=0.0374 ** (Male) and p=0.9075 (Female)

Fovea Depth vs. AL/CR: p=0.8133 (Male) and p=0.6601 (Female)

The age-based comparison looked at correlations between foveal width/depth and AL/CR separately for the two age groups (7-8 years and 10-11 years). The p-values of 0.2264 and 0.2078 indicate no significant correlation between foveal width or depth and AL/CR in either age group.

The gender-based comparison assessed correlations for males and females separately. For foveal width vs. AL/CR, there was a significant correlation in males (p=0.0374) but not in females (p=0.9075). This suggests a relationship between foveal width and AL/CR in males but not females. The correlation coefficient for males indicates that the relationship is moderately positive. As AL/CR increases, foveal width also tends to increase. This suggests that males with relatively longer axial lengths and flatter corneas (higher AL/CR ratios) tend to have wider foveal widths. In contrast, the lack of correlation in females means that foveal width appears independent of AL/CR in females. Wider foveas are not necessarily associated with specific biometric profiles in females. For foveal depth vs. AL/CR, no significant correlation was found between males (p=0.8133) or females (p=0.6601).

5 Discussion

This study analyzed foveal morphology and outer retinal layer thickness in healthy Norwegian children aged 7-11. No significant differences in foveal width, depth, or outer nuclear layer (ONL) thickness were found between males and females or between the younger (7-8 years) and older (10-11 years) cohorts. However, axial length was significantly longer in males compared to females.

Outer Retinal layer Thickness

No significant difference in outer nuclear layer (ONL) thickness at the fovea was found between males and females in this study (males 97.59 ± 9.62 μm, females 99.28 ± 10.29 μm, p=0.455). This agrees with prior research, which has generally not identified sex-related disparities in ONL thickness between males and females (Czepita et al., 2016; D. J. Lee et al., 2018; Tick et al., 2011).

Axial Length

The results revealed a significantly longer axial length in males. The longer axial length in males agrees with known sex-dependent divergence in childhood ocular growth, as males tend to have longer eyes (Li et al., 2015; Ojaimi et al., 2005; Rozema, 2023; Tideman et al., 2018). The lack of significant difference in axial length between the 7-8 and 10-11-year-old cohorts was a surprising result that requires deeper analysis. Prior longitudinal studies have consistently shown that axial length undergoes steady elongation throughout later childhood and adolescence (Hagen et al., 2019; Rozema, 2023). A longitudinal study by Hagen et al. in adolescents from age 16 to 18 showed there is a modest increase in AL was compensated by a small decrease in mean crystalline lens power (-0.064 ± 0.291D) and deepening of the anterior chamber (+0.028 ± 0.040 mm), concluding that emmetropic and low hyperopic eyes continue exhibiting slow coordinated growth (Hagen et al., 2019).

Similarly, (Li et al., 2015) used partial coherence interferometry to measure axial length in Chinese children. They reported axial elongation rates of 0.1mm/year from 6-12 years old, gradually slowing to 0.05mm/year by age 18. Another study (Tideman et al., 2018) examined axial length (AL) growth in European children aged 6, 9, and 15 years and adults around age 57. AL increased steadily from ages 6 to 15 in both boys and girls. In boys, the median AL was 22.59 mm at age 6 and 23.87 mm at adulthood, reflecting an increase of 1.28 mm. In girls, the median AL was 22.03 mm at age 6 and 23.38 mm at adulthood, an increase of 1.35 mm. In contrast, the current study of Norwegian children found a mean axial length of 22.78 mm in the 7-8-year-old cohort and 22.98 mm in the 10-11-year-old group. One potential explanation is ethnic variation in childhood ocular development and that the study is based

on cross-sectional data. Prior studies have examined African, Caucasian, or East Asian populations. However, the sample size was relatively small and narrow in age range. The study needs expansion with larger cohorts across younger ages and a longitudinal study to confirm if the axial elongation rate truly slows sooner.

Spherical equivalent refraction and Axial length/corneal radios ratio

The AL/CR ratio is important clinically because it represents the optical properties and shape of the eye. This drives the determination of the appropriate corrective lens prescription to optimize visual performance.

We observed a negative correlation between the two variables when plotting the spherical equivalent refraction (SER) against the axial length/corneal radius (AL/CR) ratio. This indicates that SER decreases as the AL/CR ratio increases. An intriguing finding was the significant correlation between foveal width and axial length/corneal radius (AL/CR) ratio exclusively in males ($p=0.0374$). As AL/CR increased in males, foveal width also tended to increase. This relationship was not observed in females, suggesting that ocular biometrics in males may influence foveal width. Given the importance of AL/CR in determining refractive correction, this finding could have clinical implications.

The relationship between foveal width and axial length/corneal radius (AL/CR) ratio in males but not females also merits further analysis. This sex difference suggests that the interplay between anatomical characteristics may influence foveal morphology in a sex-dependent manner. How other parameters like genetics, environment, and lifestyle factors affect foveal development requires extensive investigation.

Foveal Width and Potential Clinical Implications

The foveal pit diameter relates to cone photoreceptors' density and packing geometry in the central retina. Wider foveal pits are associated with lower cone densities compared to narrower pits that enable tighter packing (Tick et al., 2011). Wider foveal widths, as we observed in males with higher AL/CR ratios, could impact acuity by reducing the cone density. Clinically, this raises the question of whether optical interventions that modify retinal magnification could help compensate for wider foveal pits. For example, rigid contact lenses that reshape the corneal curvature also minify the retinal image and increase effective cone density (Plainis et al., 2011).

The correlation found here requires validation in larger studies across broader age ranges. However, this initial finding indicates a potential interaction between foveal morphology, optical biometry, and prescription correction, specifically in male children.

For clinical care to be optimized, it will be critical to understand these complex links between anatomical development, optical characteristics, and functional vision.

OCT

The role of OCT in pediatric retinal assessment has been proven in many of the studies presented in this master's thesis. One of the main focuses of this master thesis is to provide a base for normative data in the pediatric Norwegian population, as discussed in previous chapters. This thesis's OCT data and segmentation provide valuable insights into the foveal morphology and outer retinal layer thickness in a healthy Norwegian pediatric population. There are new perspectives on how the OCT can help assess the foveal morphology and how we can implement it in further analysis:

- Foveal Avascular Zone in Normal Chinese Adults

A study by Dong et al. (2022) described the morphological characteristics of the foveal avascular zone (FAZ) in normal Chinese adults with or without myopia. The study found a high variability in FAZ configuration. It revealed that females had a larger FAZ than males, which is an interesting finding, as gender-based differences in retinal structures are not extensively documented (Dong et al., 2022). In an interesting way, compared to normal people, all myopic people displayed decreased FAZ area and perimeter. These findings may be of particular importance to our study because males were found to have significantly larger axial lengths, which may impact the FAZ.

- Sub-foveal Choroidal Thickness in Pediatric Population

Enhanced depth OCT is used to evaluate the sub-foveal choroidal thickness. In the thesis, almost all the study subjects were hyperope, and the sub-foveal choroidal thickness has been a point of interest in the myope population (Al Marshood et al., 2023; Muthusamy et al., 2023). While this thesis did not focus on choroidal thickness, the importance of establishing normative data for various ocular parameters could be integrated into future research to provide a more comprehensive understanding of foveal morphology in pediatric Norwegian populations.

- Foveal morphology in assessing retinal diseases

A collective of a number of well-defined normal characteristics for foveal morphology can be used to provide an initial point of reference to compare pathological changes to. For instance, the foveal morphology may be altered in conditions like foveal hypoplasia, macular degeneration, or retinopathy of prematurity. For example, a recent study focused on the morphology of foveal hypoplasia and described the presence of hyporeflective zones in the Henle fiber layer (HFL) of eyes with high-grade foveal hypoplasia (Bringmann et al., 2022). The study classified foveal hypoplasia into high-grade and low-grade based on the thickness of the inner retinal layers. This classification could be useful in this master thesis to differentiate between varying degrees of foveal development or abnormalities.

Key findings

Understanding population-specific maturation patterns could be important for identifying abnormal growth linked to pediatric ocular conditions. This study provides initial information about axial length in Norwegians compared to reported patterns in other ethnicities.

The lack of sex differences in foveal dimensions agrees with previous studies, which found no significant difference in foveal pit shape between males and females (Wagner-Schuman et al., 2011). However, the longer axial length in males is consistent with known sex-related ocular growth disparities that emerge in childhood (Ojaimi et al., 2005; Rozema, 2023).

In summary, this study provides initial normative pediatric data on foveal anatomy in Norwegian children. The lack of major structural changes from 7-11 years suggests earlier stabilization of foveal dimensions. However, larger longitudinal studies across younger ages and diverse populations and incorporating additional biometric data are imperative to elucidate developmental patterns fully. This will strengthen our understanding of normal foveal maturation versus potential abnormalities linked to visual disorders.

The study's results are limited in their generalizability and should be validated in larger samples. However, the finding that axial length was the only parameter exhibiting a significant difference between age groups agrees with other pediatric studies (Li et al., 2015). This supports the validity of using axial length as a key biomarker of ocular growth in this age range.

6 Conclusion

This study assessed the foveal shape and outer retinal layer thickness in Norwegian children aged 7-11. The key research questions were:

1. Is there any difference in foveal shape between males and females?

2. Is there any difference in outer retinal layer thickness between males and females?

3. Do foveal shape and outer retinal layer thickness change from ages 7-8 to 10-11 years?

The results revealed no significant differences in foveal width, depth, or outer nuclear layer (ONL) thickness between males and females or between the younger (7-8 years) and older (10-11 years) cohorts. However, axial length was significantly longer in males compared to females.

The lack of sex differences in foveal morphology aligns with prior studies showing no significant foveal pit shape differences between males and females (Wagner-Schuman et al., 2011). The longer axial length in males also agrees with known sex-related divergence in childhood ocular growth patterns, as males tend to have longer eyes (Li et al., 2015; Ojaimi et al., 2005; Rozema, 2023; Tideman et al., 2018).

The absence of a significant difference in axial length between the 7-8 and 10-11-year-old groups contrasts with previous longitudinal research indicating steady axial elongation throughout later childhood, gradually slowing around age 13 (Hagen et al., 2019; Li et al., 2015; Rozema, 2023). However, the small sample size limits generalizability. Expanded cohorts across younger ages could confirm whether axial elongation slows sooner in Norwegians (longitudinal study). Understanding population-specific growth patterns will help identify abnormal development linked to pediatric eye disorders.

Compared to research indicating ongoing remodeling until adolescence in Caucasians, the lack of significant changes in foveal morphology from ages 7-8 to 10-11 suggests that primary structural maturation may occur before age 7 (Dubis et al., 2012). This underscores the need to analyze younger children to delineate the earliest phases of foveal development.

The small age range also prevents clarifying the entire developmental pathway, which is an important limitation. Additional limitations include measuring only axial length for

magnification correction rather than incorporating other biometric data to refine optical modeling (Bengtsson & Krakau, 1992; Bennett et al., 1994; Garway-Heath et al., 1998).

Future longitudinal studies with larger samples across broader age ranges are recommended. Combining axial length with more biometric data will enable sophisticated analysis of optical magnification for precise measurements of anatomical foveal morphology. Tracking individuals over time can elucidate developmental patterns and distinguish normal variation versus potential abnormal changes.

In conclusion, this study provides initial normative pediatric data on foveal structure in Norwegian children aged 7 to 11. The findings suggest earlier stabilization of foveal dimensions compared to other populations. However, ongoing research with expanded cohorts could give a better understanding of early ocular developmental patterns and their functional implications.

References/bibliography

Abràmoff, M. D., Mullins, R. F., Lee, K., Hoffmann, J. M., Sonka, M., Critser, D. B., Stasheff, S. F., & Stone, E. M. (2013). Human Photoreceptor Outer Segments Shorten During Light Adaptation. *Investigative Ophthalmology & Visual Science*, *54*(5), 3721–3728. https://doi.org/10.1167/iovs.13-11812

Ahn, H.-C., Son, H.-W., Kim, J. S., & Lee, J. H. (2005). Quantitative Analysis of Retinal Nerve Fiber Layer Thickness of Normal Children and Adolescents. *Korean Journal of Ophthalmology*, *19*(3), 195–200. https://doi.org/10.3341/kjo.2005.19.3.195

Al Marshood, A., Caso, M. J. R., AlSaedi, A., Almarek, F., Khandekar, R. B., Semidey, V. A., & Caso, M. R. (2023). Optical Coherence Tomography Based Choroidal Thickness and Its Determinants in Healthy Saudi Population: A Cross-Sectional Study. *Cureus*, *15*(1).

Albert, C., Fortune, B., Yang, H., & Gardiner, S. K. (2018). Comparison between Heidelberg Spectralis OCT1 vs OCT2 measurements in glaucomatous eyes. *Investigative Ophthalmology & Visual Science*, *59*(9), 4084.

Anwar, S., Nath, M., Gottlob, I., & Proudlock, F. A. (2023). Severity of cystoid macular oedema in preterm infants observed using hand-held spectral domain optical coherence tomography improves weekly with postmenstrual age. *Eye*, *37*(14), Article 14. https://doi.org/10.1038/s41433-023-02461-8

Asefzadeh, B., Cavallerano, A. A., & Fisch, B. M. (2007). Racial Differences in Macular Thickness in Healthy Eyes. *Optometry and Vision Science*, *84*(10).

Baraas, R. C., Pedersen, H. R., Knoblauch, K., & Gilson, S. J. (2022). Human Foveal Cone and RPE Cell Topographies and Their Correspondence With Foveal Shape. *Investigative Ophthalmology & Visual Science*, *63*(2), 8–8. https://doi.org/10.1167/iovs.63.2.8

Barak, Y., Sherman, M. P., & Schaal, S. (2011). Mathematical Analysis of Specific Anatomic

Foveal Configurations Predisposing to the Formation of Macular Holes. *Investigative Ophthalmology & Visual Science*, *52*(11), 8266–8270. https://doi.org/10.1167/iovs.11-8191

Bengtsson, B., & Krakau, C. E. T. (1992). Correction of optic disc measurements on fundus photographs. *Graefe's Archive for Clinical and Experimental Ophthalmology*, *230*(1), 24–28. https://doi.org/10.1007/BF00166758

Bennett, A. G., Rudnicka, A. R., & Edgar, D. F. (1994). Improvements on Littmann's method of determining the size of retinal features by fundus photography. *Graefe's Archive for Clinical and Experimental Ophthalmology*, *232*(6), 361–367. https://doi.org/10.1007/BF00175988

Bonnin, S., Sandali, O., Bonnel, S., Monin, C., & El Sanharawi, M. (2015). Vitrectomy with internal limiting membrane peeling for tractional and nontractional diabetic macular edema: Long-term Results of a Comparative Study. *RETINA*, *35*(5), 921. https://doi.org/10.1097/IAE.0000000000000433

Boulton, M., & Dayhaw-Barker, P. (2001). The role of the retinal pigment epithelium: Topographical variation and ageing changes. *Eye*, *15*(3), Article 3. https://doi.org/10.1038/eye.2001.141

Brezinski, M. E. (2006). *Optical Coherence Tomography: Principles and Applications*. Elsevier Science & Technology. http://ebookcentral.proquest.com/lib/ucsn-ebooks/detail.action?docID=274698

Bringmann, A., Barth, T., & Ziemssen, F. (2022). Morphology of foveal hypoplasia: Hyporeflective zones in the Henle fiber layer of eyes with high-grade foveal hypoplasia. *PLOS ONE*, *17*(4), e0266968. https://doi.org/10.1371/journal.pone.0266968

Bringmann, A., Pannicke, T., Grosche, J., Francke, M., Wiedemann, P., Skatchkov, S. N., Osborne, N. N., & Reichenbach, A. (2006). Müller cells in the healthy and diseased retina. *Progress in Retinal and Eye Research*, *25*(4), 397–424.

https://doi.org/10.1016/j.preteyeres.2006.05.003

Bringmann, A., Syrbe, S., Görner, K., Kacza, J., Francke, M., Wiedemann, P., & Reichenbach, A. (2018). The primate fovea: Structure, function and development. *Progress in Retinal and Eye Research*, *66*, 49–84. https://doi.org/10.1016/j.preteyeres.2018.03.006

Bruce, A., Pacey, I. E., Bradbury, J. A., Scally, A. J., & Barrett, B. T. (2013). Bilateral Changes in Foveal Structure in Individuals with Amblyopia. *Ophthalmology*, *120*(2), 395–403. https://doi.org/10.1016/j.ophtha.2012.07.088

Carlson, M. D. A., & Morrison, R. S. (2009, January 27). *Study Design, Precision, and Validity in Observational Studies* (140 Huguenot Street, 3rd Floor New Rochelle, NY 10801-5215 USA) [Research-article]. Https://Home.Liebertpub.Com/Jpm; Mary Ann Liebert, Inc. 140 Huguenot Street, 3rd Floor New Rochelle, NY 10801-5215 USA. https://doi.org/10.1089/jpm.2008.9690

Chang, J. W. (2019). Risk factor analysis for the development and progression of retinopathy of prematurity. *PLoS ONE*, *14*(7), e0219934. https://doi.org/10.1371/journal.pone.0219934

Chui, T. Y. P., Zhong, Z., Song, H., & Burns, S. A. (2012). Foveal Avascular Zone and Its Relationship to Foveal Pit Shape. *Optometry and Vision Science*, *89*(5), 602–610. https://doi.org/10.1097/OPX.0b013e3182504227

Cook, C., Sulik, K. K., & Wright, K. W. (2003). *Pediatric Ophthalmology and Strabismus*.

Curcio, C. A., Sloan, K. R., Kalina, R. E., & Hendrickson, A. E. (1990). Human photoreceptor topography. *Journal of Comparative Neurology*, *292*(4), 497–523. https://doi.org/10.1002/cne.902920402

Czepita, M., Machalińska, A., & Cholewa, M. (2016). Macular outer plexiform layer and outer nuclear layer thickness on spectral domain optical coherence tomography in central serous chorioretinopathy—A case of two patients. *Ophthalmology Journal*, *1*(2), Article 2. https://doi.org/10.5603/OJ.2016.0011

Demir, P., Hovsepian, N., Pagels, P., Petersson, V., Baskaran, K., & Macedo, A. F. (2022). All retinas are not created equal: Fovea-to-macula thickness ratio and foveal microvasculature in healthy young children. *Ophthalmic and Physiological Optics*, *42*(3), 644–652. https://doi.org/10.1111/opo.12958

Dong, Y.-M., Zhu, H.-Y., Liu, Z.-H., Fu, S.-Y., Wang, K., Du, L.-P., & Jin, X.-M. (2022). Various configuration types of the foveal avascular zone with related factors in normal Chinese adults with or without myopia assessed by swept-source OCT angiography. *International Journal of Ophthalmology*, *15*(9), 1502–1510. https://doi.org/10.18240/ijo.2022.09.14

Dubis, A. M., Hansen, B. R., Cooper, R. F., Beringer, J., Dubra, A., & Carroll, J. (2012). Relationship between the foveal avascular zone and foveal pit morphology. *Investigative Ophthalmology & Visual Science*, *53*(3), 1628–1636. https://doi.org/10.1167/iovs.11-8488

El-Dairi, M. A., Asrani, S. G., Enyedi, L. B., & Freedman, S. F. (2009). Optical Coherence Tomography in the Eyes of Normal Children. *Archives of Ophthalmology*, *127*(1), 50–58. https://doi.org/10.1001/archophthalmol.2008.553

Evans, B. (2009). Binocular vision assessment. *Optometry: Science, Techniques and Clinical Management. Edinburgh: Butterworth-Heinemann*, 241–256.

Fagerland, M. W. (2012). t-tests, non-parametric tests, and large studies—A paradox of statistical practice? *BMC Medical Research Methodology*, *12*(1), 78. https://doi.org/10.1186/1471-2288-12-78

Finn, A. P., House, R. J., Hsu, S. T., Thomas, A. S., El, -Dairi Mays A., Freedman, S., Materin, M. A., & Vajzovic, L. (2019). Hyperreflective Vitreous Opacities on Optical Coherence Tomography in a Patient With Bilateral Retinoblastoma. *Ophthalmic Surgery, Lasers and Imaging Retina*, *50*(1), 50–52. https://doi.org/10.3928/23258160-20181212-08

Fox, J. (2016). *Using the R Commander: A Point-and-Click Interface for R*. CRC Press.

Garway-Heath, D. F., Rudnicka, A. R., Lowe, T., Foster, P. J., Fitzke, F. W., & Hitchings, R. A. (1998). Measurement of optic disc size: Equivalence of methods to correct for ocular magnification. *British Journal of Ophthalmology*, *82*(6), 643–649. https://doi.org/10.1136/bjo.82.6.643

Hagen, L. A., Gilson, S. J., Akram, M. N., & Baraas, R. C. (2019). Emmetropia Is Maintained Despite Continued Eye Growth From 16 to 18 Years of Age. *Investigative Ophthalmology & Visual Science*, *60*(13), 4178–4186. https://doi.org/10.1167/iovs.19-27289

Hasegawa, T., Ueda, T., Okamoto, M., & Ogata, N. (2014). Relationship between presence of foveal bulge in optical coherence tomographic images and visual acuity after rhegmatogenous retinal detachment repair. Retina, *34*(9), 1848. https://doi.org/10.1097/IAE.0000000000000160

Hendrickson, A. E., & Yuodelis, C. (1984). The Morphological Development of the Human Fovea. *Ophthalmology*, *91*(6), 603–612. https://doi.org/10.1016/S0161-6420(84)34247-6

Hendrickson, A., Possin, D., Vajzovic, L., & Toth, C. A. (2012). Histologic development of the human fovea from midgestation to maturity. *Am J Ophthalmol*, *154*(5), 767-778.e2. https://doi.org/10.1016/j.ajo.2012.05.007

Hildebrand, G. D., & Fielder, A. R. (2011). Anatomy and Physiology of the Retina. In J. Reynolds & S. Olitsky (Eds.), *Pediatric Retina* (pp. 39–65). Springer. https://doi.org/10.1007/978-3-642-12041-1_2

Hoshi, H., Liu, W.-L., Massey, S. C., & Mills, S. L. (2009). ON Inputs to the OFF Layer: Bipolar Cells That Break the Stratification Rules of the Retina. *The Journal of Neuroscience*, *29*(28), 8875–8883. https://doi.org/10.1523/JNEUROSCI.0912-09.2009

Iannetti, L., Scarinci, F., Alisi, L., Armentano, M., Sampalmieri, L., La Cava, M., & Gharbiya, M. (2023). Correlation between Morphological Characteristics of Macular Edema and

Visual Acuity in Young Patients with Idiopathic Intermediate Uveitis. *Medicina*, *59*(3), 529. https://doi.org/10.3390/medicina59030529

Kanski, J. J. (2015). *Kanski's Clinical Ophthalmology, 8th Edition* (Saunders Ltd, Ed.). Elsevier.

Kelty, P. J., Payne, J. F., Trivedi, R. H., Kelty, J., Bowie, E. M., & Burger, B. M. (2008). Macular Thickness Assessment in Healthy Eyes Based on Ethnicity Using Stratus OCT Optical Coherence Tomography. *Investigative Ophthalmology & Visual Science*, *49*(6), 2668–2672. https://doi.org/10.1167/iovs.07-1000

Kiernan, D. F., Mieler, W. F., & Hariprasad, S. M. (2010). Spectral-Domain Optical Coherence Tomography: A Comparison of Modern High-Resolution Retinal Imaging Systems. *American Journal of Ophthalmology*, *149*(1), 18-31.e2. https://doi.org/10.1016/j.ajo.2009.08.037

Killingsworth, M. C., Sarks, J. P., & Sarks, S. H. (1990). Macrophages related to Bruch's membrane in age-related macular degeneration. *Eye*, *4*(4), 613–621.

Landa, G., Gentile, R. C., Garcia, P. M. T., Muldoon, T. O., & Rosen, R. B. (2012). External limiting membrane and visual outcome in macular hole repair: Spectral domain OCT analysis. *Eye*, *26*(1), 61–69.

Larsen, J. S. (1971). The Sagittal Growth of the Eye. *Acta Ophthalmologica*, *49*(6), 873–886. https://doi.org/10.1111/j.1755-3768.1971.tb05939.x

Lee, D. J., Woertz, E. N., Visotcky, A., Wilk, M. A., Heitkotter, H., Linderman, R. E., Tarima, S., Summers, C. G., Brooks, B. P., Brilliant, M. H., Antony, B. J., Lujan, B. J., & Carroll, J. (2018). The Henle Fiber Layer in Albinism: Comparison to Normal and Relationship to Outer Nuclear Layer Thickness and Foveal Cone Density. *Investigative Ophthalmology & Visual Science*, *59*(13), 5336–5348. https://doi.org/10.1167/iovs.18-24145

Lee, E. K., & Yu, H. G. (2015). Ganglion Cell–Inner Plexiform Layer and Peripapillary Retinal Nerve Fiber Layer Thicknesses in Age-Related Macular Degeneration. *Investigative*

Ophthalmology & Visual Science, *56*(6), 3976–3983. https://doi.org/10.1167/iovs.15-17013

Lee, H., Purohit, R., Patel, A., Papageorgiou, E., Sheth, V., Maconachie, G., Pilat, A., McLean, R. J., Proudlock, F. A., & Gottlob, I. (2015). In Vivo Foveal Development Using Optical Coherence Tomography. *Investigative Ophthalmology & Visual Science*, *56*(8), 4537–4545. https://doi.org/10.1167/iovs.15-16542

Lee, J. W. Y., Yau, G. S. K., Woo, T. T. Y., & Lai, J. S. M. (2015). The Association Between Macular Thickness and Peripapillary Retinal Nerve Fiber Layer Thickness in Chinese Children. *Medicine*, *94*(8), e567. https://doi.org/10.1097/MD.0000000000000567

Levin, L. A., Nilsson, S. F. E., Hoeve, J. V., Wu, S., Kaufman, P. L., & Alm, A. (2011). *Adler's Physiology of the Eye: Expert Consult - Online and Print*. Elsevier Health Sciences.

Li, S.-M., Wang, N., Zhou, Y., Li, S.-Y., Kang, M.-T., Liu, L.-R., Li, H., Sun, Y.-Y., Meng, B., Zhan, S.-Y., & Atchison, D. A. (2015). Paraxial Schematic Eye Models for 7- and 14-Year-Old Chinese Children. *Investigative Ophthalmology & Visual Science*, *56*(6), 3577–3583. https://doi.org/10.1167/iovs.15-16428

Mann, C. J. (2003). Observational research methods. Research design II: Cohort, cross sectional, and case-control studies. *Emergency Medicine Journal*, *20*(1), 54–60. https://doi.org/10.1136/emj.20.1.54

Marmor, M. F. (1999). Retinal and retinal pigment epithelial physiology. *Vitreoretinal Disease: The Essentials. Thieme Medical Publishers, Inc., New York*, 25–38.

Matsui, Y., Miyata, R., Uchiyama, E., Matsubara, H., & Kondo, M. (2020). Misalignment of foveal pit and foveal bulge determined by ultrahigh-resolution SD-OCT in normal eyes. *Graefe's Archive for Clinical and Experimental Ophthalmology*, *258*(10), 2131–2139. https://doi.org/10.1007/s00417-020-04813-6

Menghini, M., Lujan, B. J., Zayit-Soudry, S., Syed, R., Porco, T. C., Bayabo, K., Carroll, J., Roorda, A., & Duncan, J. L. (2015). Correlation of outer nuclear layer thickness with cone density values in patients with retinitis pigmentosa and healthy subjects.

Investigative Ophthalmology & Visual Science, *56*(1), 372–381.

Mirhajianmoghadam, H., Jnawali, A., Musial, G., Queener, H. M., Patel, N. B., Ostrin, L. A., & Porter, J. (2020). In vivo assessment of foveal geometry and cone photoreceptor density and spacing in children. *Sci Rep*, *10*(1), 8942. https://doi.org/10.1038/s41598-020-65645-2

Mishra, A., Wong, A., Bizheva, K., & Clausi, D. A. (2009). Intra-retinal layer segmentation in optical coherence tomography images. *Optics Express*, *17*(26), 23719–23728. https://doi.org/10.1364/OE.17.023719

Muthusamy, S., Balaji, J. J., Parithala, A., & Lakshminarayanan, V. (2023). Measurement of sub-foveal choroidal thickness from optical low coherence reflectometry biometry: A new method. *Ophthalmic Technologies XXXIII*, *12360*, 133–139.

Ogden, T. E. (1983). Nerve fiber layer of the macaque retina: Retinotopic organization. *Investigative Ophthalmology & Visual Science*, *24*(1), 85–98.

Ojaimi, E., Rose, K. A., Morgan, I. G., Smith, W., Martin, F. J., Kifley, A., Robaei, D., & Mitchell, P. (2005). Distribution of Ocular Biometric Parameters and Refraction in a Population-Based Study of Australian Children. *Investigative Ophthalmology & Visual Science*, *46*(8), 2748–2754. https://doi.org/10.1167/iovs.04-1324

Pedersen, H. R., Baraas, R. C., Landsend, E. C. S., Utheim, Ø. A., Utheim, T. P., Gilson, S. J., & Neitz, M. (2020). PAX6 Genotypic and Retinal Phenotypic Characterization in Congenital Aniridia. *Investigative Ophthalmology & Visual Science*, *61*(5), 14–14. https://doi.org/10.1167/iovs.61.5.14

Plainis, S., Petratou, D., Giannakopoulou, T., Atchison, D. A., & Tsilimbaris, M. K. (2011). Binocular summation improves performance to defocus-induced blur. *Investigative Ophthalmology & Visual Science*, *52*(5), 2784–2789. https://doi.org/10.1167/iovs.10-6545

Provis, J. M. (2001). Development of the Primate Retinal Vasculature. *Progress in Retinal and Eye Research*, *20*(6), 799–821. https://doi.org/10.1016/S1350-9462(01)00012-X

Provis, J. M., Dubis, A. M., Maddess, T., & Carroll, J. (2013). Adaptation of the central retina for high acuity vision: Cones, the fovea and the avascular zone. *Progress in Retinal and Eye Research*, *35*, 63–81. https://doi.org/10.1016/j.preteyeres.2013.01.005

Radius, R. L., & Anderson, D. R. (1979). The Histology of Retinal Nerve Fiber Layer Bundles and Bundle Defects. *Archives of Ophthalmology*, *97*(5), 948–950. https://doi.org/10.1001/archopht.1979.01020010506027

Raviv, S., Bharti, K., Rencus-Lazar, S., Cohen-Tayar, Y., Schyr, R., Evantal, N., Meshorer, E., Zilberberg, A., Idelson, M., Reubinoff, B., Grebe, R., Rosin-Arbesfeld, R., Lauderdale, J., Lutty, G., Arnheiter, H., & Ashery-Padan, R. (2014). PAX6 Regulates Melanogenesis in the Retinal Pigmented Epithelium through Feed-Forward Regulatory Interactions with MITF. *PLOS Genetics*, *10*(5), e1004360. https://doi.org/10.1371/journal.pgen.1004360

Raynor, W., Mangalesh, S., Sarin, N., & Toth, C. A. (2021). Foveal Development in Retinopathy of Prematurity. In W.-C. Wu & W.-C. Lam (Eds.), *A Quick Guide to Pediatric Retina* (pp. 123–134). Springer. https://doi.org/10.1007/978-981-15-6552-6_16

Reynolds, J. D., & Olitsky, S. E. (2010). *Pediatric Retina*. Springer Science & Business Media.

Rozema, J. J. (2023). Refractive development I: Biometric changes during emmetropisation. *Ophthalmic and Physiological Optics*, *43*(3), 347–367. https://doi.org/10.1111/opo.13094

Samara, W. A., Say, E. A. T., Khoo, C. T. L., Higgins, T. P., Magrath, G., Ferenczy, S., & Shields, C. L. (2015). Correlation of foveal avascular zone size with foveal morphology in normal eyes using optical coherence tomography angiography. Retina, *35*(11), 2188. https://doi.org/10.1097/IAE.0000000000000847

Sasaki, K., Sasaki, K., Hirota, M., Hayashi, T., & Mizota, A. (2022). Comparisons of size of foveal avascular zone area among children with posterior microphthalmos, high

hyperopia, and normal eyes. *International Ophthalmology*, *42*(8), 2599–2607. https://doi.org/10.1007/s10792-022-02250-4

Scheibe, P., Lazareva, A., Braumann, U.-D., Reichenbach, A., Wiedemann, P., Francke, M., & Rauscher, F. G. (2013). Parametric model for the 3D reconstruction of individual fovea shape from OCT data. *Experimental Eye Research*, *119*, 26. http://dx.doi.org/10.1016/j.exer.2013.11.008

Schmitt, J. M. (1999). Optical coherence tomography (OCT): A review. *IEEE Journal of Selected Topics in Quantum Electronics*, *5*(4), 1205–1215. https://doi.org/10.1109/2944.796348

Seresirikachorn, K., Thiamthat, W., Aramtiantamrong, N., Traichaiyaporn, S., Wanichwecharungruang, B., Patel, N. A., & Vu, D. M. (2023). Two types of childhood glaucoma secondary to familial exudative vitreoretinopathy. *Journal of American Association for Pediatric Ophthalmology and Strabismus*, *27*(4), 192.e1-192.e8. https://doi.org/10.1016/j.jaapos.2023.05.006

Sommer, A., Miller, N. R., Pollack, I., Maumenee, A. E., & George, T. (1977). The Nerve Fiber Layer in the Diagnosis of Glaucoma. *Archives of Ophthalmology*, *95*(12), 2149–2156. https://doi.org/10.1001/archopht.1977.04450120055003

SPECTRALIS OCT - The modular Imaging Platform | Heidelberg Engineering. (n.d.). Retrieved September 25, 2023, from https://business-lounge.heidelbergengineering.com/us/en/products/spectralis/spectralis/#product-details

Staurenghi, G., Sadda, S., Chakravarthy, U., & Spaide, R. F. (2014). Proposed Lexicon for Anatomic Landmarks in Normal Posterior Segment Spectral-Domain Optical Coherence Tomography: The IN•OCT Consensus. *Ophthalmology*, *121*(8), 1572–1578. https://doi.org/10.1016/j.ophtha.2014.02.023

Suncin A., M. A. (2022). *Structural and shape changes on the fovea and outer retinal layers in Norwegian children ages 7-8 to 10-11.*

Tan, P. E. Z., Yu, P. K., Balaratnasingam, C., Cringle, S. J., Morgan, W. H., McAllister, I. L., & Yu, D.-Y. (2012). Quantitative confocal imaging of the retinal microvasculature in the human retina. *Investigative Ophthalmology & Visual Science*, *53*(9), 5728–5736. https://doi.org/10.1167/iovs.12-10017

Testa, F., Surace, E. M., Rossi, S., Marrocco, E., Gargiulo, A., Di Iorio, V., Ziviello, C., Nesti, A., Fecarotta, S., Bacci, M. L., Giunti, M., Corte, M. della, Banfi, S., Auricchio, A., & Simonelli, F. (2011). Evaluation of Italian Patients with Leber Congenital Amaurosis due to AIPL1 Mutations Highlights the Potential Applicability of Gene Therapy. *Investigative Ophthalmology & Visual Science*, *52*(8), 5618–5624. https://doi.org/10.1167/iovs.10-6543

Thomas, M. G., Papageorgiou, E., Kuht, H. J., & Gottlob, I. (2022). Normal and abnormal foveal development. *British Journal of Ophthalmology*, *106*(5), 593–599. https://doi.org/10.1136/bjophthalmol-2020-316348

Tick, S., Rossant, F., Ghorbet, I., Gaudric, A., Sahel, J.-A., Chaumet-Riffaud, P., & Paques, M. (2011). Foveal Shape and Structure in Normal Population. *Investigative Ophthalmology and Visual Science*, *52*(8).

Tideman, J. W. L., Polling, J. R., Vingerling, J. R., Jaddoe, V. W. V., Williams, C., Guggenheim, J. A., & Klaver, C. C. W. (2018). Axial length growth and the risk of developing myopia in European children. *Acta Ophthalmologica*, *96*(3), 301–309. https://doi.org/10.1111/aos.13603

Vajzovic, L., Hendrickson, A. E., O'Connell, R. V., Clark, L. A., Tran-Viet, D., Possin, D., Chiu, S. J., Farsiu, S., & Toth, C. A. (2012). Maturation of the human fovea: Correlation of spectral-domain optical coherence tomography findings with histology. *Am J Ophthalmol*, *154*(5), 779-789.e2. https://doi.org/10.1016/j.ajo.2012.05.004

Van Buren, E., & Herring, A. H. (2020). To be parametric or non-parametric, that is the question. *BJOG: An International Journal of Obstetrics & Gynaecology*, *127*(5), 549–550. https://doi.org/10.1111/1471-0528.15545

van den Burg, G. J. J., Nazábal, A., & Sutton, C. (2019). Wrangling messy CSV files by detecting row and type patterns. *Data Mining and Knowledge Discovery*, *33*(6), 1799–1820. https://doi.org/10.1007/s10618-019-00646-y

Ventura, L. M., Sorokac, N., Santos, R. D. L., Feuer, W. J., & Porciatti, V. (2006). The Relationship between Retinal Ganglion Cell Function and Retinal Nerve Fiber Thickness in Early Glaucoma. *Investigative Ophthalmology & Visual Science*, *47*(9), 3904–3911. https://doi.org/10.1167/iovs.06-0161

Wagner-Schuman, M., Dubis, A. M., Nordgren, R. N., Lei, Y., Odell, D., Chiao, H., Weh, E., Fischer, W., Sulai, Y., Dubra, A., & Carroll, J. (2011). Race- and sex-related differences in retinal thickness and foveal pit morphology. *Invest Ophthalmol Vis Sci*, *52*(1), 625–634. https://doi.org/10.1167/iovs.10-5886

Wang, Y., Bensaid, N., Tiruveedhula, P., Ma, J., Ravikumar, S., & Roorda, A. (2019). *Human foveal cone photoreceptor topography and its dependence on eye length*. https://doi.org/10.7554/elife.47148

Wilkinson, C. P., Hinton, D. R., Sadda, S. R., & Wiedemann, P. (2017). *Ryan's Retina: 3 Volume Set*. Elsevier Health Sciences.

Won, J. Y., Kim, S. E., & Park, Y.-H. (2016). Effect of age and sex on retinal layer thickness and volume in normal eyes. *Medicine*, *95*(46), e5441. https://doi.org/10.1097/MD.0000000000005441

Wu, Y., Thibos, L. N., & Candy, T. R. (2018). Two-dimensional simulation of eccentric photorefraction images for ametropes: Factors influencing the measurement. *Ophthalmic and Physiological Optics*, *38*(4), 432–446. https://doi.org/10.1111/opo.12563

Wurtz, R. H., Kandel, E. R., Schwartz, J. H., & Messel, T. M. (2000). Principles of neural science. *Kande ER, Schwartz JH, Jessell TM. Central Visual Pathways. 4th Ed. New York (NY): McGraw-Hill*, 523–547.

Wylegala, E. (2011). Technical principles of optical coherence tomography and basic

differences among time-domain, spectral-domain and swept-source OCT. *Acta Ophthalmologica*, *89*(s248), 0–0. https://doi.org/10.1111/j.1755-3768.2011.4131.x

Yuodelis, C., & Hendrickson, A. (1986). A qualitative and quantitative analysis of the human fovea during development. *Vision Research*, *26*(6), 847–855. https://doi.org/10.1016/0042-6989(86)90143-4

List of tables and charts

Attachments

- Information letters

Are you interested in taking part in the research project

Structural and shape changes on the fovea and outer retinal layers in Norwegian children from ages 7-8 to 10-11

This is an inquiry about participation in a research project where the main purpose is to assess foveal shape and outer retinal layer thickness in children aged 7-8 and 10-11 who grow up in Norway. In this letter we will give you information about the purpose of the project and what your participation will involve.

Purpose of the project
The objective of this study is to assess the foveal shape and outer retinal layer thickness in children aged 7-8 and 10-11 who grow up in Norway.
The research questions are helping us answer the following questions:
Is there any difference in the foveal shape between boys and girls from Norway?
Is there any difference in the outer retinal layer thickness in boys and girls from Norway?
Do foveal shape and outer retinal layer thickness change from ages 7-8 to 10-11?

The final results of this study will give us a better understanding of how the fovea develops in children growing up in Norway.

Who is responsible for the research project?
The University of South-eastern Norway is the institution responsible for the project.

Why are you being asked to participate?
The subjects are girls and boys who have grown up in Norway from ages 7 to 11. They will be divided into two groups (7 to 8 and 10 to 11 years old). The images acquired will be part of the study conducted by researchers in the Colour Vision and Retinal Imaging Laboratory at the University of South-Eastern Norway.

The study sample will consist of about 80 participants, about equal number of boys and girls.

What does participation involve for you?
If you choose to be part of the project, this will involve that the image taken will be part of a database in the USN. The information collected will be stored safely and anonymized electronically. You will have access to the data that is collected in this study. The procedure of taking the image of the retina of the children is quick and painless; a minimum grade of attention is needed to take the pictures. The parents/guardians can be with the children in the whole process.

Participation is voluntary
Participation in the project is voluntary. If you choose to participate, you can withdraw your consent at any time without giving a reason. All information about you will then be made anonymous. There will be no negative consequences for you if you choose not to participate or later decide to withdraw.

The voluntary withdrawal from this study will not affect your present or future treatment at the USN.

Your personal privacy – how we will store and use your personal data
We will only use your personal data for the purpose(s) specified in this information letter. We will process your personal data confidentially and in accordance with data protection legislation (the General Data Protection Regulation and Personal Data Act).

- The data is stored in a safe electronic location at the Colour Vision and Retinal Imaging Laboratory at the University of South-Eastern Norway. Only the principal investigator and project manager will have access to the images.
- I will replace your name and contact details with a random code. The list of names, contact details, and respective codes will be stored separately from the rest of the collected data. The data will be stored in a safe electronic location.

The personal information will not be published.

What will happen to your personal data at the end of the research project?
The project is scheduled to end July 2024. At the end, all the data collected will be stored for future research. The random codes assigned to identify the images will be deleted.

Your rights
So long as you can be identified in the collected data, you have the right to:

- access the personal data that is being processed about you
- request that your personal data be deleted
- request that incorrect personal data about you be corrected/rectified
- receive a copy of your personal data (data portability), and
- send a complaint to the Data Protection Officer or The Norwegian Data Protection Authority regarding the processing of your personal data

What gives us the right to process your personal data?
We will process your personal data based on your consent.

Based on an agreement with the University of South-Eastern Norway. Data Protection Services has assessed that the processing of personal data in this project is in accordance with data protection legislation.

Where can I find out more?
If you have questions about the project or want to exercise your rights, contact:

- University of South-Eastern Norway via Rigmor C. Baraas by email Rigmor.Baraas@usn.no
- Our Data Protection Officer: postmottak@usn.no
- Data Protection Services, by email: (personverntjenester@sikt.no) or by telephone: +47 53 21 15 00.

Yours sincerely,

Project Leader

Student

Rigmor C. Baraas

Arturo Suncin

(Researcher/supervisor)

(Project Manager)

Consent form

I have received and understood information about the project Structural and shape changes on the fovea and outer retinal layers in Norwegian children from ages 7-8 to 10-11 and have been given the opportunity to ask questions. I give consent:

- □ for my/my child to participate in this study
- □ to take images of my child's retina

I give consent for my personal data to be processed until the end date of the project, approx. July 2024

(Signed by participant, date)

- Norwegian Centre for Research Data (NSD)

NSD NORSK SENTER FOR FORSKNINGSDATA

Notification Form

Reference number

665489

Which personal data will be processed?

- Date of birth
- Health data

Project information

Project title

Structural and shape changes on the fovea and outer retinal layers in Norwegian children from ages 7-8 to 10-11

Project description

The objective of this study is to assess the foveal shape and outer retinal layer thickness in children aged 7-8 and
10-11 who grow up in Norway.
The research questions that helped formulate the objective of this study were:
Is there any difference in the foveal shape between boys and girls from Norway?
Is there any difference in the outer retinal layer thickness in boys and girls from Norway?
Do foveal shape and outer retinal layer thickness change from ages 7-8 to 10-11?
The final results of this study will give us a better understanding of how the fovea develops in children growing up in Norway.

Explain why the processing of personal data is necessary.

The data collected in this project is limited to the birth date of each participant. Name, address, or any personal information is not needed/relevant for this project. The pictures that are going to be analyzed are already taken and anonymized.

External funding

Type of project

Student project, Master's thesis

Contact information, student

Mauricio Arturo Suncin Aguilar, arsun86@proton.me, tlf: 41333720

Data controller

Data controller (institution responsible for the project)

Universitetet i Sørøst-Norge / Fakultet for helse- og sosialvitenskap / Institutt for optometri, radiografi og lysdesign

Project leader (academic employee/supervisor or PhD candidate)

Rigmor Baraas, Rigmor.Baraas@usn.no, tlf: +4792836659

Will the responsibility of the data controller be shared with other institutions (joint data controllers)?

No

Sample 1

Describe the sample

Children with healthy eyes between 7 and 11 years old.

Recruitment or selection of the sample

The pictures to analyze in this study are already taken by the institution (USN).

Age

7 - 11

Will you include adults (18 years and over) who do not have the capacity to consent?

No

Personal data relating to sample 1

- Date of birth
- Health data

How will you collect data relating to sample 1?

Data from another research project

Legal basis for processing general categories of personal data

Consent (art. 6 nr. 1 a)

Who will give consent for children under 16 years?

Parents/guardians

Legal basis for processing special categories of personal data

Explicit consent (art. 9 nr. 2 a)

Explain your choice of legal basis

Information for sample 1

Will you inform the sample about the processing of their personal data?

No

Explain why you will not inform the sample about the processing of their personal data.

The initial collection of data has been explained orally and written to every parent/guardian and children, and they have fully accepted to use of the data in other projects.

Third Persons

Will you be processing data relating to third persons?

No

Documentation

How will consent be documented?

Manually (on paper)

How can consent be withdrawn?

The subject can withdraw their consent either orally or in writing. An oral withdrawal can be personally or done by a phone call.

How can data subjects get access to their personal data or have their personal data corrected or deleted?

The subject has already access to their personal data through the open service of the USN.

Total number of data subjects in the project

1-99

Approvals

Will you obtain any of the following approvals or permits for the project?

Processing

Where will the personal data be processed?

Computer belonging to the data controller

Who will be processing/have access to the collected personal data?

Student (student project)

Will the collected personal data be transferred/made available to a third country or international organisation outside the EU/EEA?

No

Information Security

Will directly identifiable data be stored separately from the rest of the collected data (e.g., in a scrambling key)?

Yes

Which technical and practical measures will be used to secure the personal data?

Personal data will be anonymized as soon as no longer needed.

Duration of processing

Project period

01.08.2022 - 22.12.2023

Will personal data be stored after the end of the project?

No, the collected data will be stored in anonymous form.

Which anonymization measures will be taken?

Personally identifiable information will be removed, re-written, or categorized.

Will the data subjects be identifiable (directly or indirectly) in the thesis/publications from the project?

No

Additional information

https://meldeskjema.nsd.no/eksport/6290bf16-9f2e-4229-910a-de8861ee9eea

- Raw data

Group	sex	fovea width in microns	fovea depth in microns	ONL thickness at fovea in microns	axial length in mm	cr in mm	SER in diopters	AL/cr
Age 7 to 8	female	2098	136	107	22,913961	8,088574409484860	2,22	2,83288004
Age 7 to 8	female	1961	119	105	22,600080	8,133436203002930	2,26	2,778663216
Age 7 to 8	female	2175	100	102	23,134730	7,812775135040280	1,44	2,961141157
Age 7 to 8	female	2609	122	100	22,412119	8,030483245849610	1,68	2,790880488
Age 7 to 8	female	2504	123	109	23,331543	8,195795059204100	1,66	2,846769939
Age 7 to 8	female	2301	101	99	23,015196	7,825237274169920	1,01	2,941149922
Age 7 to 8	female	1990	140	98	22,943697	7,806353569030760	0,99	2,939105537
Age 7 to 8	female	2385	117	90	23,011185	7,633088111877440	0,99	3,014662567
Age 7 to 8	female	2302	88	127	23,327078	7,976004600524900	0,92	2,924657039
Age 7 to 8	female	2356	127	100	22,427265	7,607263565063470	2,27	2,948113829

Age 7 to 8	female	2408	111	104	22,709460	7,668528079986570	0,63	2,961384475
Age 7 to 8	female	2089	144	92	22,144135	7,501040458679190	1,34	2,952141789
Age 7 to 8	female	2226	126	108	21,981152	7,852190494537350	2,14	2,799365606
Age 7 to 8	female	2126	129	99	22,483765	7,887802124023430		2,850447393
Age 7 to 8	female	2253	128	90	22,959110	7,774000167846680	1,95	2,953319977
Age 7 to 8	female	2321	121	88	21,630083	7,403512001037590	0,65	2,921597614
Age 7 to 8	female	2347	106	95	22,106396	7,931128501892090	2,38	2,787295149
Age 7 to 8	female	2542	108	79	22,934448	7,843095302581780		2,924157761
Age 7 to 8	female	2519	133	96	21,933700	7,538367271423340		2,909608833
Age 7 to 8	female	2276	132	102	22,221280	8,072923660278320	2,61	2,752569073
Age 7 to 8	male	2421	111	108	21,790611	7,870391368865960	3,49	2,768682011
Age 7 to 8	male	2132	124	91	22,313921	7,460951328277580	0,98	2,990760832

Age 7 to 8	male	2263	120	96	23,226763	7,935115814208980	0,79	2,92708557
Age 7 to 8	male	2408	123	99	22,111965	7,415371894836420	0,68	2,981909109
Age 7 to 8	male	1682	113	96	22,598969	7,520680427551260	0,65	3,004910156
Age 7 to 8	male	2139	165	88	22,213718	7,671483993530270	1,65	2,895622023
Age 7 to 8	male	2265	137	90	22,685630	7,805900573730460	1,46	2,906215598
Age 7 to 8	male	2487	143	105	21,757130	7,529592514038080	1,51	2,889549462
Age 7 to 8	male	2367	106	91	22,718401	7,878937244415280	1,87	2,883434694
Age 7 to 8	male	2298	126	93	23,163965	7,642391204833980	1,04	3,030983939
Age 7 to 8	male	2545	71	77	24,351282	8,266031265258780	1,00	2,945946031
Age 7 to 8	male	2136	122	103	22,483082	7,581954956054680	2,04	2,965341014
Age 7 to 8	male	2499	136	113	23,921875	8,177607536315910	1,01	2,925290177
Age 7 to 8	male	2370	121	97	23,810688	8,248928070068360	1,78	2,886519048

Age 7 to 8	male	2239	166	98	23,308784	7,794686317443840	1,13	2,990342786
Age 7 to 8	male	2199	85	87	24,225613	8,445966720581050	0,93	2,868305524
Age 7 to 8	male	2497	142	101	22,412422	7,767027854919430	1,91	2,885585377
Age 7 to 8	male	2224	111	122	23,883282	8,179235458374020	0,32	2,919989542
Age 7 to 8	male	2163	138	107	23,238098	7,597518920898430	0,09	3,058642991
Age 7 to 8	male	2132	110	93	23,401707	7,446291923522940	−0,67	3,142732952
Age 7 to 8	male	2286	70	74	22,122440	7,615454673767090	1,82	2,904940144
Age 10 to 11	female	2012	95	112	21,935690	7,260350227355950	0,54	3,021299154
Age 10 to 11	female	2276	105	111	23,904583	8,148363113403320	0,80	2,933666881
Age 10 to 11	female	2280	94	82	22,323402	7,536065101623530	1,17	2,962209283
Age 10 to 11	female	2360	136	91	22,096748	7,481609344482420	1,16	2,953475246

Age 10 to 11	female	2727	126	112	23,048603	7,846883296966550	1,03	2,937293971
Age 10 to 11	female	2215	142	90	22,640295	7,728220939636230	0,30	2,929561043
Age 10 to 11	female	2158	114	94	22,250355	7,829727172851560	2,65	2,841779095
Age 10 to 11	female	2443	128	110	22,656220	7,722822189331050	0,84	2,933671065
Age 10 to 11	female	2410	132	99	23,303144	7,713146209716790	0,78	3,021224202
Age 10 to 11	female	2200	116	94	22,874762	7,852946281433100	0,85	2,912889148
Age 10 to 11	female	2365	133	109	23,027077	7,779199600219720	0,70	2,960083066
Age 10 to 11	female	1963	125	93	22,195066	7,577096462249750	0,93	2,929203102
Age 10 to 11	female	2281	134	90	22,875896	7,666767120361320	2,01	2,983773426
Age 10 to 11	female	2727	143	93	22,489600	7,774651527404780	1,35	2,892682704

Age 10 to 11	female	2114	117	104	21,809190	7,32683086 3952630	1,27	2,9766 19824
Age 10 to 11	female	2228	127	102	22,174528	7,29136466 9799800	0,59	3,0412 04082
Age 10 to 11	female	2448	139	92	22,236963	7,57496929 1687010	0,70	2,9355 84574
Age 10 to 11	female	2646	113	121	23,845850	8,20198440 5517570	1,04	2,9073 26913
Age 10 to 11	female	2189	166	83	22,789850	7,87517690 6585690	1,28	2,8938 84197
Age 10 to 11	male	2153	148	94	23,207615	7,74216270 4467770	1,07	2,9975 62294
Age 10 to 11	male	2651	149	94	23,967371	7,96485996 2463370	0,74	3,0091 39032
Age 10 to 11	male	2271	142	104	24,541270	8,13311195 3735350	0,21	3,0174 51394
Age 10 to 11	male	2294	130	83	24,039377	7,62517976 7608640	−0,20	3,1526 30854
Age 10 to 11	male	2225	106	93	22,122725	7,34828519 8211670	0,70	3,0105 96949

Age 10 to 11	male	2241	103	102	23,512580	7,848051548004150	0,80	2,995976754
Age 10 to 11	male	2327	129	101	24,063390	8,179746627807610	1,46	2,941825841
Age 10 to 11	male	2470	110	104	23,267286	8,153616905212400	0,90	2,853615306
Age 10 to 11	male	2611	138	95	23,692247	7,971045494079590	0,56	2,972288518
Age 10 to 11	male	1829	93	107	24,101528	7,661890506744380	−1,14	3,145637226
Age 10 to 11	male	1919	143	117	22,645094	7,872588157653800	2,44	2,87644845
Age 10 to 11	male	2425	155	90	21,239342	7,758018493652340	5,67	2,737727684
Age 10 to 11	male	2483	121	99	23,550772	8,007605552673340	1,29	2,941050461
Age 10 to 11	male	1968	153	101	23,077202	7,752147674560540	0,64	2,976878533
Age 10 to 11	male	2117	118	93	23,460918	7,709428787231440	0,45	3,043146081

Age 10 to 11	male	1935	109	102	23,852790	8,01112747 1923820	1,06	2,9774 57303
Age 10 to 11	male	2195	146	94	23,358774	8,12187004 0893550	2,73	2,8760 33953
Age 10 to 11	male	2439	103	104	22,177662	7,54564762 1154780		2,9391 33009